

A near-infrared catalogue of the Galactic novae in the VVV survey area[★]

R. K. Saito^{1,2,3}, D. Minniti^{1,3,4,5}, R. Angeloni^{1,3,6}, M. Catelan^{1,3}, J. C. Beamin^{1,3}, J. Borissova^{2,3}, I. Dékány^{1,3},
E. Kerins⁷, R. Kurtev², and R. E. Mennickent⁸

¹ Departamento de Astronomía y Astrofísica, Pontificia Universidad Católica de Chile, Av. Vicuña Mackenna 4860, 782-0436 Macul, Santiago, Chile

² Departamento de Física y Astronomía, Facultad de Ciencias, Universidad de Valparaíso, Ave. Gran Bretaña 1111, Playa Ancha, Casilla 5030, Valparaíso, Chile

³ The Milky Way Millennium Nucleus, Av. Vicuña Mackenna 4860, 782-0436 Macul, Santiago, Chile

⁴ Vatican Observatory, Vatican City State V-00120, Italy

⁵ Departamento de Ciencias Físicas, Universidad Andres Bello, Av. Republica 252, Santiago, Chile

⁶ Department of Electrical Engineering, Center for Astro-Engineering, Pontificia Universidad Católica de Chile, Av. Vicuña Mackenna 4860, 782-0436 Macul, Santiago, Chile

⁷ Jodrell Bank Centre for Astrophysics, University of Manchester, Oxford Road, Manchester M13 9PL, UK

⁸ Departamento de Astronomía, Universidad de Concepción, Casilla 160-C, Concepción, Chile

Received ; Accepted

ABSTRACT

Context. Near-infrared data of Classical Novae contain useful information about the ejected gas mass and the thermal emission by dust formed during eruption, and provide independent methods to classify the objects according to the colour of their progenitors, and the fading rate and features seen after eruption. The VISTA Variables in the Vía Láctea survey (VVV) is a near-IR ESO Public Survey mapping the Milky Way bulge and southern plane. Data taken during 2010 – 2011 covered the entire area in the JHK_s bands plus some epochs in K_s -band of the ongoing VVV variability campaign.

Aims. We used the VVV data to create a near-IR catalogue of the known Galactic novae in the 562 sq. deg. area covered by VVV. We also compiled the information about novae from the variability tables of the VVV variability campaign.

Methods. We used the novae list provided by VSX/AAVSO catalogue to search for all objects within the VVV area. From the 140 novae, we were able to retrieve the JHK_s colours of 93 objects. We also checked in the ongoing VVV variability campaign for the light-curves of novae that erupted in the last years.

Results. The VVV near-IR catalogue of novae contains JHK_s photometry of 93 objects completed as of December 2012. VVV allows to monitor objects within up to $\Delta K_s \sim 10$ mag range. VVV images can also be used to discover and study novae by searching for the expanding shell. Since objects are seen at different distances and reddening levels, the colour-magnitude and colour-colour diagrams show the novae spread in magnitude as well as in colour. Dereddened colours and reddening-free indices were used with caution and cannot be a good approach in all cases since the distance and spectral features prevent more conclusive results for some extreme objects. Light-curves for some recent novae are presented.

Conclusions. Thanks to its high spatial resolution in the near-IR, and large K_s -range, the VVV survey can be a major contributor for the search and study of novae in the most crowded and high-extinction regions of the Milky Way. The VVV survey area contains $\sim 35\%$ of all known novae in the Galaxy.

Key words. Stars: novae, cataclysmic variables – Galaxy: stellar content – Catalogs – Surveys

1. Introduction

Cataclysmic variable stars (CVs) are close binary systems composed by a late-type star which transfers material to a more massive white dwarf (WD) companion. The typical mass transfer rates in CVs are $10^{-8} - 10^{-11} M_{\odot} \text{ yr}^{-1}$, and the progressive accretion of hydrogen-rich material from the secondary star onto the hot surface of the WD can lead to a thermonuclear runaway, in which the accreted material is expelled from the system. This phenomenon is a so called nova eruption (e.g., Frank et al. 2002; Warner 2003).

During a nova eruption the object suddenly rises in brightness, becoming typically 8-15 magnitudes brighter than its progenitor. The recurrence between nova outbursts is expected to be $10^3 - 10^6$ years, and depends on the mass of the white dwarf and the mass transfer rate. The systems are classified as Classical Novae when just one nova eruption was recorded. However, this is strongly biased by ancient records, which are limited to a few thousand years. Systems with two or more registered nova eruptions are classified as Recurrent Novae, in general associated with a high-mass transfer rate system onto a primary star with the mass close to the Chandrasekhar limit (Warner 2003).

Since novae are usually found in eruption, the novae classification is in general based on the features seen during this phase, such as the fading (speed class) rate after the nova eruption (e.g.,

Send offprint requests to: R. K. Saito: rsaito@astro.puc.cl

[★] Based on observations taken within the ESO VISTA Public Survey VVV, Programme ID 179.B-2002

Gaposchkin 1957) and the spectral differences (e.g., Williams 1992).

More recently, alternative classifications are proposed based either on the Galactic component, with disk and bulge novae (e.g., della Valle & Livio 1998), or using automated selection and classification based on optical photometry (Darnley et al. 2004).

The infrared light can also contain the thermal emission by dust formed during the shell ejection. Models for thermonuclear runaway predict the presence of material from the white dwarf in the ejecta, thus its spectroscopic analysis allows to distinguish between CO and ONe white dwarfs (Shafter et al. 2011). The importance of observing Galactic novae in the IR spectral region was fully understood when it was realized that they can represent a significant contributor to the interstellar medium (at least on local scales) of highly processed material, thus playing an active role in the chemical evolution of the Galaxy. Furthermore, IR observations provide independent methods for determining the ejected gas mass, a key parameter of every thermonuclear runaway model (Mason et al. 1998).

IR data can also help in the determination both of the global Galactic nova rate and the separate Galactic bulge and disk nova rates. Current Galactic nova samples, obtained mostly from optical surveys, are biased towards regions of lower optical extinction and therefore are incomplete within both the bulge and disk towards the Galactic plane. Previous determinations of the Galactic nova rate therefore vary by more than an order of magnitude, from 11 to 260 yr⁻¹ (Shafter 1997). The nova rate in M31 is better constrained from optical studies (e.g., Darnley et al. 2006) but it remains unclear whether the rates within both galaxies are consistent with fixed bulge and disk nova rates per unit galactic luminosity. Again this uncertainty is due mostly to the poorly constrained knowledge of the Galactic rate. A large scale near-infrared time domain survey can allow novae to be identified throughout the Galactic bulge and disk and therefore facilitate a more complete determination of the nova rate within each stellar population.

The VISTA Variables in the Vía Láctea is a ESO Public near-IR survey scanning the Milky Way (MW) bulge and southern plane, in five near-IR bands (*ZYJHK_s*), plus a variability campaign of about 100 epochs in the *K_s*-band spanning over many years (Minniti et al. 2010). VVV is about four magnitudes deeper than previous IR surveys, and thanks to its higher spatial resolution in the near-IR, enables deep observations in the most crowded and high-extinction regions of the Milky Way (e.g., Saito et al. 2012a).

Here we present a catalogue with the *JHK_s* colours of 93 novae in the VVV area. We discuss the colour properties and features seen in the near-IR. We also present the first results from the VVV variability campaign, including light-curves for some novae. VVV can be a major contributor for the discovery and study of novae in the innermost regions of the Galaxy, objects that are beyond detection in the current novae searches.

2. Observations

VVV is an ESO Public Survey observing the MW bulge and inner southern plane in the near-IR with the VISTA Telescope located at Cerro Paranal Observatory in Chile (Minniti et al. 2010, and references therein). VVV observes an area of about 562 deg², within $-10.0^\circ \leq l \leq +10.5^\circ$ and $-10.3^\circ \leq b \leq +5.1^\circ$ in the bulge, and within $294.7^\circ \leq l \leq 350.0^\circ$ and $-2.25^\circ \leq b \leq +2.25^\circ$ in the plane (see Fig. 1). The whole bulge and disk areas were fully observed in five near-IR passbands (*ZYJHK_s*) during

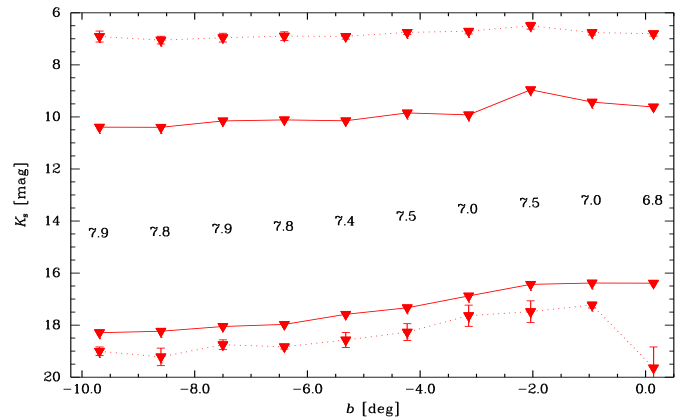


Fig. 2. Magnitude range covered by the VVV *K_s*-band variability campaign observations along the Galactic minor axis. The solid lines with triangles mark the limits covered by the stellar sources, with the value of the total magnitude range shown in each position. The increasing sky brightness towards the Galactic centre is due to the contribution of the underlying, unresolved faint stars. The upper dotted line with triangles shows the mean value of the brightest sources, including objects flagged as saturated. Similarly, the lower dotted line with triangles marks the limiting magnitude of all sources, including those below the 5- σ limit.

2010–2011, while a variability campaign in the *K_s*-band is ongoing, with ~ 100 pointings planned over many years (Saito et al. 2012a).

Photometric catalogues for the VVV observations are provided by the Cambridge Astronomical Survey Unit (CASU)¹. The catalogues contain the positions, fluxes, and some shape measurements obtained from different apertures, with a flag indicating the most probable morphological classification. The VVV data are in the natural VISTA Vegamag system, with the photometric calibration in *JHK_s* performed using the VISTA magnitudes of unsaturated 2MASS stars present in the images. The single-band CASU catalogues for each tile were matched, creating a *JHK_s* catalogue of more than 173 million sources in the VVV bulge area (Saito et al. 2012b), and about 148 million sources in the disk. A similar procedure was adopted to match the *K_s*-band catalogues from the variability campaign in order to create variability tables for selected fields.

Different observing strategies between the bulge and disk area, and effects caused by crowding and extinction cause both the limiting magnitude and saturation to vary along the VVV area (Saito et al. 2012a,b). For instance, the *K_s*-band limiting magnitude on the outer bulge is about 18.5 mag, while in the Galactic center the limit is *K_s* ~ 16.5 mag (see Fig. 2). The saturation limit varies in a shorter range. The *JHK_s* observations for a given field were taken in the same “observational block” (OB) which guarantees quasi-simultaneous observations in the three bands (there is a time gap of only ~ 190 s between each band). On the other hand, due to multiple scheduling constraints on the side of the VISTA telescope operations, there is a little control on the cadence of the *K_s*-band variability data within a given season, with the number of epochs planned in a given year being observed together with the other VISTA surveys according with the surveys requirements on the weather and visibility, for instance.

¹ <http://casu.ast.cam.ac.uk/vistasp/>

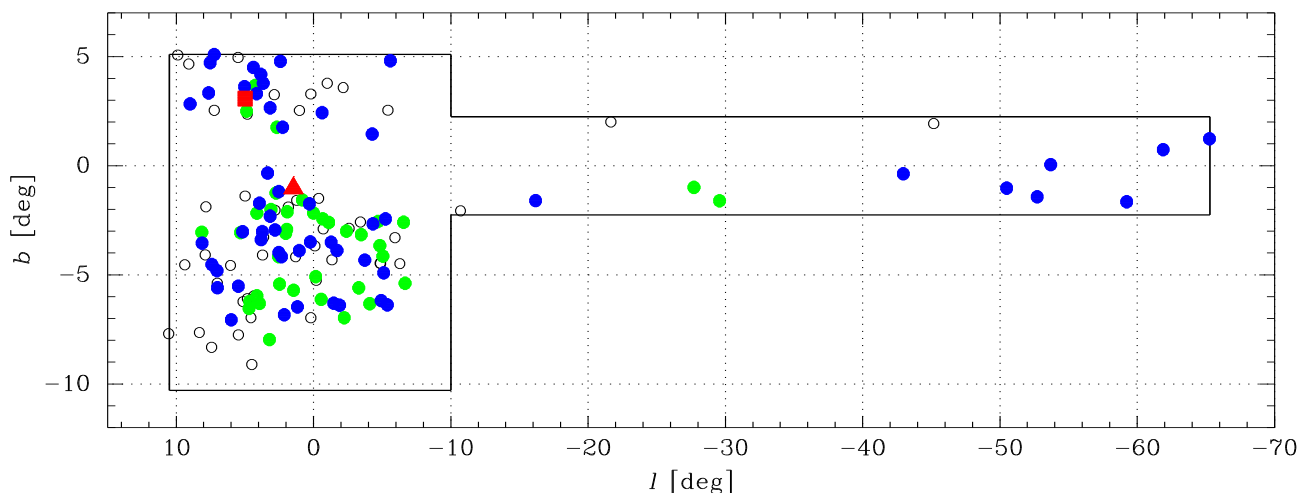


Fig. 1. Spatial distribution of all known Galactic novae in the VVV survey area. A total of 140 objects are present. Filled symbols mark the objects detected in the VVV data while open symbols mark the novae with no detection in our data. The blue circles are novae with the coordinates matching a single source within $1''$ from the position given by the catalogue. Green circles mark the novae with doubtful photometry (see text). The red square is Nova Sgr 2012 progenitor, while the red triangle marks the position of Nova Sgr 2010b, caught during eruption. We note the presence of a “zone of avoidance” on the Galactic plane, with just a few objects belonging to the high-extinction regions of the MW.

3. The VVV Novae Catalogue

Our novae list was taken from The International Variable Star Index (VSX), provided by the American Association of Variable Star Observers² (AAVSO). In this catalogue there are about 400 known novae in the Galaxy, 140 of them lie within the VVV area. Fig. 1 shows their spatial distribution, with most objects concentrated towards the Galactic bulge. We note that the information about some novae are from historical records or amateur astronomers, with the coordinates in general taken from observations while the objects were in eruption. Thus, in order to certify the coordinates with enough accuracy during the quiescent state, we checked for all objects in the SIMBAD database³. Finally, we defined as our coordinates the ICRS J2000 RA and DEC taken from SIMBAD, which were used as entries in our search for the VVV JHK_s photometry and composite colour images.

² <http://www.aavso.org/vsx/index.php>

³ simbad.u-strasbg.fr/simbad/

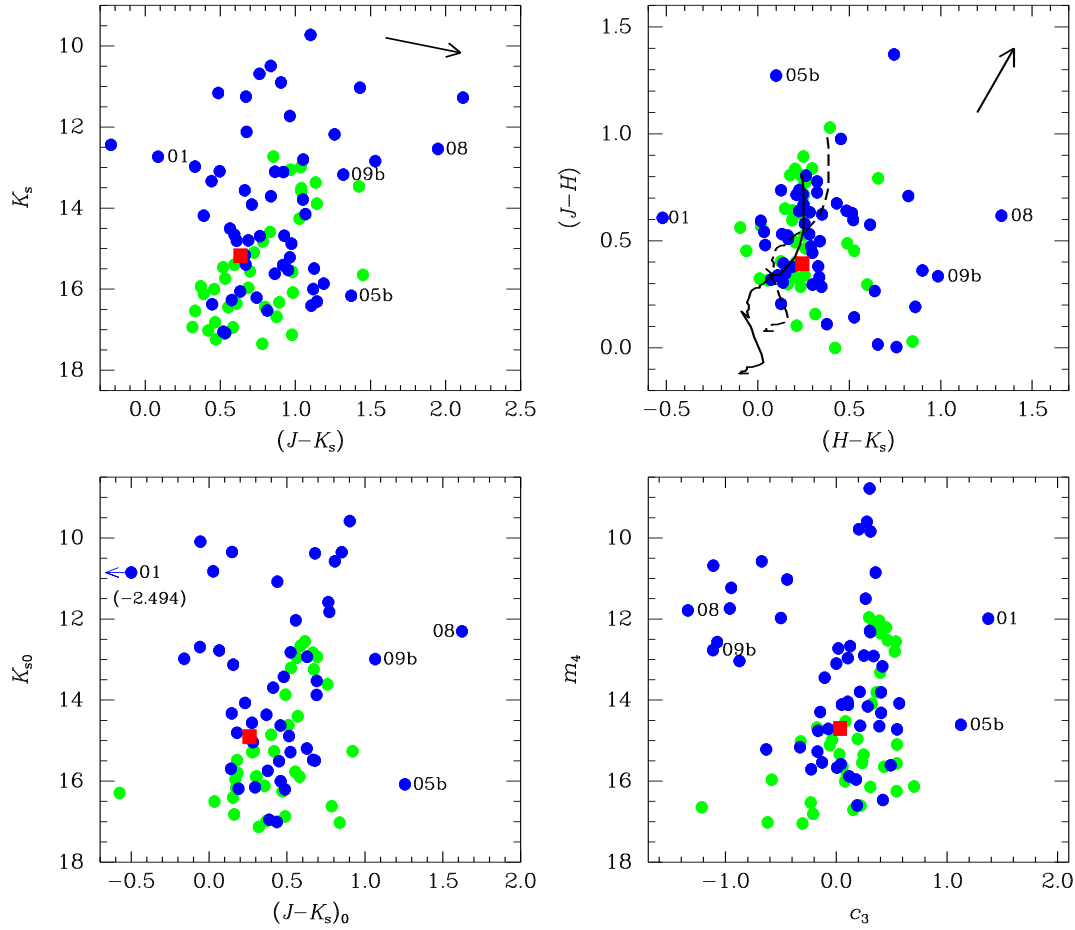


Fig. 3. Top-left panel: K_s vs. $(J-K_s)$ CMD for all novae detected in the VVV area. The colour pattern and symbols are the same as used in Fig. 1. Top-right panel: the corresponding $(J-H)$ vs. $(H-K_s)$ colour-colour diagram. Bottom-left: dereddened CMD for all bulge Novae, using the reddening maps of Gonzalez et al. (2012) and assuming the Cardelli et al. (1989) extinction law (no disk novae are plotted). Bottom-right: CMD using the reddening-free parameters provided by Catelan et al. (2011). The colour of main sequence stars is shown in the $(J-H)$ vs. $(H-K_s)$ CCD in the case of $A_{K_s} = 0$ mag (no extinction, solid line) and for $A_{K_s} = 0.243$ (the median value of extinction among our targets, shown as a dashed line; adapted from Ducati et al. 2001). The reddening vector associated with an extinction of $E(B-V) = 1$, based on the relative extinctions of the VISTA filters, and assuming the Cardelli et al. (1989) extinction law, is also shown in the top panels. Four objects are labelled in the plots: Nova Sgr 2001, Nova Sgr 2005b, Nova Sgr 2008, and Nova Sgr 2009b.

Table 1. Previously known novae in the VVV area (completed as of December 2012). We adopted the novae type designations described by VSX database¹: Novae (N), subdivided into fast (NA), slow (NB), and very slow (NC) categories. The coordinates (epoch J2000) were taken from Simbad². The distance between the Simbad coordinates and the VVV source is presented. Values of extinction (A_{K_s}) are for a 2 arcmin region around the target position, taken from the maps of Gonzalez et al. (2012). The abbreviations used in the last column are MS (multiple sources), ND (no detection) and ST (saturated source). The “:” symbol stands for doubtful sources (see text).

Nova (Year)	Other Designation	Nova Type	RA [hh:mm:ss.ss]	DEC [dd:mm:ss.s]	RA (VVV) [hh:mm:ss.ss]	DEC (VVV) [dd:mm:ss.ss]	Dist. ["]	J [mag]	H [mag]	K_s [mag]	A_{K_s} [mag]	Note
Sgr 1893	V5557 Sgr	N	18:01:43.15	-35:39:27.8	18:01:43.14	-35:39:28.95	1.155	17.528±0.076	16.959±0.093	16.943±0.154	0.070	MS
Sgr 1897	LQ Sgr	NA	18:28:28.91	-27:55:19.2	—	—	—	—	—	—	—	ST
Sgr 1899	V1016 Sgr	NA	18:19:57.63	-25:11:14.6	18:19:57.63	-25:11:14.52	0.089	11.329±0.010	10.749±0.010	10.493±0.010	0.113	
Sco 1901	V0382 Sco	NA	17:51:56.13	-35:25:05.4	—	—	—	—	—	—	—	ND
Sgr 1901	V1014 Sgr	NB	18:06:45.70	-27:26:15.0	—	—	—	—	—	—	—	ND
Sgr 1905	V1015 Sgr	NA	18:09:02.00	-32:28:32.0	18:09:02.06	-32:28:30.84	1.407	17.250±0.063	17.147±0.102	16.935±0.154	0.112	MS:
Cir 1906	AR Cir	NB	14:48:09.53	-60:00:27.5	14:48:09.52	-60:00:27.69	0.204	12.211±0.010	12.701±0.010	12.439±0.010	—	
Sco 1906	V0711 Sco	NB	17:54:06.16	-34:21:15.5	17:54:06.16	-34:21:15.55	0.070	13.967±0.010	13.328±0.010	13.103±0.010	0.171	
Sgr 1910	V0999 Sgr	NB	18:00:05.59	-27:33:14.0	—	—	—	—	—	—	—	ND
Sgr 1914c	V1012 Sgr	NA	18:06:14.00	-31:44:27.0	18:06:14.10	—	—	—	—	—	—	ND
Sgr 1917	BS Sgr	NB:	18:26:46.72	-27:08:19.9	18:26:46.72	-27:08:19.84	0.061	12.795±0.010	12.286±0.010	12.120±0.010	0.087	
Sgr 1919	V1017 Sgr	NA+UG	18:32:04.17	-29:23:12.6	—	—	—	—	—	—	—	ND
Sco 1922	V0707 Sco	N	17:48:26.38	-36:37:54.9	—	—	—	—	—	—	—	ND
Sgr 1924	FL Sgr	NA	18:00:30.20	-34:36:13.0	18:00:30.27	-34:36:11.99	1.353	17.710±0.159	17.553±0.242	17.239±0.260	0.111	MS:
Sgr 1926	FM Sgr	NA	18:17:18.10	-23:38:27.0	18:17:18.05	-23:38:27.30	0.787	16.819±0.082	16.481±0.115	16.373±0.144	0.187	MS
Sgr 1926a	KY Sgr	NA	18:01:21.02	-26:24:40.0	18:01:21.02	-26:24:39.95	0.073	11.804±0.010	11.539±0.010	10.900±0.010	0.551	
Sco 1928	KP Sco	NA	17:44:16.47	-35:43:23.6	—	—	—	—	—	—	—	ND
Sgr 1928	V1583 Sgr	NA	18:15:26.30	-23:23:18.0	18:15:26.27	-23:23:18.95	1.020	16.998±0.094	16.637±0.129	16.445±0.151	0.277	MS:
Sgr 1930	V0441 Sgr	NA	18:22:08.09	-25:28:53.7	—	—	—	—	—	—	—	ND
Cen 1931	MT Cen	NA	11:44:00.80	-60:33:39.5	11:44:00.80	-60:33:39.55	0.050	15.607±0.010	14.892±0.010	14.681±0.010	—	
Sgr 1932	V1905 Sgr	NA	18:33:42.10	-25:20:42.0	—	—	—	—	—	—	—	ND
Sgr 1933	V0737 Sgr	N	18:07:08.66	-28:44:52.3	18:07:08.71	-28:44:52.24	0.621	15.483±0.036	14.959±0.037	14.796±0.041	0.167	MS
Cru 1935	AP Cru	NA/DQ	12:31:20.45	-64:26:25.2	12:31:20.44	-64:26:25.23	0.083	15.852±0.011	15.229±0.011	14.878±0.015	—	
Sco 1935	V0744 Sco	N:	17:53:18.08	-31:13:35.1	17:53:18.17	-31:13:35.37	1.210	17.098±0.201	16.306±0.189	15.648±0.135	0.385	MS:
Sgr 1936	V0732 Sgr	NA	17:56:07.51	-27:22:16.1	17:56:07.51	-27:22:16.36	0.261	13.391±0.010	12.020±0.010	11.275±0.010	0.922	
Sgr 1936b	V0726 Sgr	NA	18:19:33.69	-26:53:19.6	18:19:33.73	-26:53:19.66	0.591	16.484±0.048	15.748±0.045	15.621±0.059	0.143	
Sgr 1936c	V0630 Sgr	NA	18:08:48.25	-34:20:21.4	18:08:48.39	-34:20:21.70	1.723	17.557±0.051	17.528±0.109	16.682±0.106	0.064	:
Sgr 1936d	V0990 Sgr	NA	17:57:19.00	-28:19:07.0	—	—	—	—	—	—	—	ND
Sgr 1937	V0787 Sgr	NA	18:00:02.20	-30:30:31.0	18:00:02.18	-30:30:30.22	0.821	15.415±0.054	14.822±0.052	14.806±0.067	0.243	MS
Oph 1940	V0553 Oph	NA	17:42:53.50	-24:51:26.2	17:42:53.46	-24:51:25.45	0.951	16.480±0.093	15.756±0.102	15.528±0.118	0.488	MS
Sco 1941	V0697 Sco	NA/DQ	17:51:21.83	-37:24:55.2	17:51:21.91	-37:24:56.91	1.934	16.870±0.047	16.547±0.068	16.537±0.109	0.131	:
Sgr 1943	V1148 Sgr	N	18:09:05.85	-25:59:08.0	18:09:05.85	-25:59:08.06	0.065	13.308±0.010	13.103±0.010	12.976±0.010	0.285	
Sco 1944	V0696 Sco	NA	17:53:11.56	-35:50:14.4	17:53:11.55	-35:50:14.41	0.109	14.577±0.010	14.259±0.010	14.187±0.016	0.116	
Sgr 1944	V0927 Sgr	NA	18:07:42.70	-33:21:17.0	18:07:42.72	-33:21:17.77	0.805	16.846±0.042	16.304±0.049	16.270±0.082	0.065	MS
Sgr 1945a	V1149 Sgr	N	18:18:30.40	-28:17:17.0	18:18:30.37	-28:17:18.35	1.389	17.626±0.102	17.223±0.127	17.098±0.191	0.116	MS:
Sgr 1945b	V1431 Sgr	N:	18:03:29.61	-29:59:54.6	18:03:29.55	-29:59:54.84	0.852	12.692±0.010	11.975±0.010	11.729±0.010	0.144	
Sgr 1947a	V0928 Sgr	N	18:18:59.30	-28:06:00.0	—	—	—	—	—	—	—	ND
Sgr 1948	V1150 Sgr	N	18:18:55.40	-24:05:32.0	—	—	—	—	—	—	—	ND
Sco 1949	V0902 Sco	N:	17:26:08.30	-39:04:05.0	—	—	—	—	—	—	—	ND
Oph 1950	V2110 Oph	NC	17:43:33.32	-22:45:37.0	17:43:33.32	-22:45:36.95	0.074	11.647±0.010	11.537±0.010	11.160±0.010	0.336	ST

⁽¹⁾ <http://www.aavso.org/> ⁽²⁾ <http://simbad.u-strasbg.fr/simbad/>

Table 1. cont. Previously known novae in the VVV area.

Nova (Year)	Other Designation	Nova Type	RA [hh:mm:ss.ss]	DEC [dd:mm:ss.s]	RA (VVV) [hh:mm:ss.ss]	DEC (VVV) [dd:mm:ss.ss]	Dist. [']	<i>J</i> [mag]	<i>H</i> [mag]	<i>K_s</i> [mag]	<i>A_{K_s}</i> [mag]	Note
Sco 1950a	V0719 Sco	NA	17:45:43.90	-34:00:55.0	17:45:43.85	-34:00:55.41	0.724	16.179±0.070	15.442±0.067	15.216±0.068	0.328	MS:
Sco 1950b	V0720 Sco	NA	17:51:58.00	-35:23:22.0	—	—	—	—	—	—	—	ND
Sco 1950c	V0721 Sco	N	17:42:29.10	-34:40:41.5	17:42:29.10	-34:40:41.60	0.103	13.587±0.010	13.241±0.010	13.091±0.012	0.314	
Sgr 1951a	V1172 Sgr	N	17:50:23.66	-20:40:29.9	17:50:23.65	-20:40:29.88	0.114	12.460±0.010	11.484±0.010	11.030±0.010	0.454	
Sgr 1951b	V2415 Sgr	N:	17:53:12.00	-29:34:25.0	17:53:11.99	-29:34:24.39	0.629	17.053±0.293	16.478±0.329	15.864±0.242	0.371	
Sco 1952	—	n	17:47:38.00	-33:11:55.0	—	—	—	—	—	—	—	ND
Sco 1952a	V0722 Sco	NA	17:48:37.00	-34:57:50.0	17:48:36.88	-34:57:50.78	1.679	15.607±0.034	15.011±0.033	14.823±0.037	0.201	MS:
Sco 1952b	V0723 Sco	NA	17:50:05.20	-35:23:58.0	17:50:05.32	-35:23:56.79	1.939	15.422±0.028	14.780±0.029	14.591±0.030	0.191	MS:
Sgr 1952a	V1175 Sgr	NA	18:14:17.00	-31:07:08.0	18:14:17.01	-31:07:08.42	0.432	17.614±0.097	17.220±0.120	17.080±0.178	0.072	
Sgr 1952b	V1174 Sgr	N	18:01:37.00	-28:44:24.0	18:01:37.07	-28:44:22.94	1.439	14.021±0.015	13.307±0.013	13.053±0.013	0.220	:
Sgr 1953	NSV 10158	N:	18:05:12.00	-29:54:24.0	—	—	—	—	—	—	—	ND
Oph 1954	V0908 Oph	N	17:28:41.00	-27:45:24.0	—	—	—	—	—	—	—	ND
Sco 1954	NSV 9808	N:	17:53:40.00	-30:45:32.0	17:53:40.08	-30:45:31.48	1.177	15.288±0.056	14.516±0.056	14.261±0.057	0.391	:
Sgr 1954a	V1274 Sgr	NB	17:48:55.00	-17:51:55.0	—	—	—	—	—	—	—	ND
Sgr 1954b	V1275 Sgr	NA	17:59:06.35	-36:18:40.8	17:59:06.34	-36:18:40.80	0.169	14.225±0.010	13.694±0.010	13.562±0.010	0.134	
Sgr 1955	V1572 Sgr	N	18:05:37.00	-31:37:42.0	18:05:36.87	-31:37:43.02	1.894	16.506±0.053	16.053±0.064	16.116±0.106	0.162	:
Oph 1957	V0972 Oph	NB	17:34:43.81	-28:10:35.8	17:34:43.87	-28:10:36.34	0.927	17.450±0.229	16.821±0.287	16.306±0.262	0.560	
Sgr 1960	V1944 Sgr	N	18:00:36.90	-27:17:13.0	18:00:36.98	-27:17:13.70	1.320	14.550±0.027	13.743±0.025	13.510±0.026	0.268	MS:
Oph 1961	V1012 Oph	N	17:41:34.38	-23:23:33.1	17:41:34.43	-23:23:32.34	1.063	17.284±0.149	16.722±0.167	16.818±0.249	0.315	:
Sgr 1963	NSV 9828	N:	17:54:43.00	-28:41:41.0	—	—	—	—	—	—	—	ND
Sco 1964	V0825 Sco	N	17:49:53.65	-33:32:13.7	17:49:53.73	-33:32:13.13	1.194	16.259±0.076	15.766±0.096	15.561±0.101	0.298	:
Sgr 1968	V4027 Sgr	NB	18:02:29.21	-28:45:19.9	18:02:29.18	-28:45:21.23	1.403	13.582±0.010	12.954±0.010	12.728±0.010	0.174	:
Sgr 1974	V3888 Sgr	NA	17:48:41.07	-18:45:37.0	—	—	—	—	—	—	—	ND
Sgr 1975	V3889 Sgr	NA	17:58:21.32	-28:21:52.7	17:58:21.46	-28:21:53.20	1.927	15.035±0.042	14.141±0.036	13.892±0.037	0.279	MS:
Sgr 1977	V4021 Sgr	NA	18:38:14.26	-23:22:47.0	—	—	—	—	—	—	—	ND
Sgr 1978	V4049 Sgr	N	18:20:38.06	-27:56:26.0	18:20:37.99	-27:56:24.59	1.673	16.460±0.036	16.163±0.050	16.000±0.073	0.113	:
Sgr 1980	V4065 Sgr	NA	18:19:38.20	-24:43:55.9	18:19:38.22	-24:43:55.87	0.260	10.829±0.010	10.052±0.010	9.728±0.010	0.144	ST
Sgr 1982	V4077 Sgr	N	18:34:39.41	-26:26:02.9	—	—	—	—	—	—	—	ND
Nor 1983	V0341 Nor	NA	16:13:44.40	-53:19:08.0	16:13:44.23	-53:19:07.13	1.754	18.129±0.133	17.603±0.153	17.349±0.181	—	:
Oph 1983	V0794 Oph	NB	17:38:49.25	-22:50:48.9	17:38:49.25	-22:50:49.00	0.114	14.031±0.010	13.361±0.010	13.111±0.010	0.289	
Sgr 1983	V4121 Sgr	N	18:07:54.77	-28:49:26.8	18:07:54.90	-28:49:26.45	1.769	15.980±0.057	15.695±0.072	15.461±0.074	0.177	MS:
Sgr 1984	V4092 Sgr	NA	17:53:41.99	-29:02:08.4	17:53:41.91	-29:02:08.73	1.099	14.618±0.035	13.782±0.033	13.579±0.034	0.374	MS:
Sco 1985	V0960 Sco	N	17:56:34.14	-31:49:36.3	17:56:34.17	-31:49:35.55	0.830	15.216±0.037	14.412±0.033	14.149±0.034	0.274	MS
Sgr 1986	V4579 Sgr	NB	18:03:37.89	-28:00:08.9	18:03:37.90	-28:00:08.65	0.296	13.778±0.012	13.473±0.015	13.336±0.017	0.209	
Sgr 1987	V4135 Sgr	N	17:59:45.08	-32:16:20.8	—	—	—	—	—	—	—	ND
Sco 1989b	V0977 Sco	N	17:51:50.25	-32:31:58.0	17:51:50.35	-32:31:57.59	1.389	14.024±0.012	13.250±0.011	12.988±0.012	0.327	:
Cen 1991	V0868 Cen	NA	13:50:10.60	-63:08:52.0	13:50:10.69	-63:08:51.94	0.619	17.513±0.032	16.838±0.041	16.407±0.064	—	
Oph 1991b	V2290 Oph	NA	17:43:05.50	-20:07:00.0	17:43:05.47	-20:07:00.59	0.734	16.951±0.057	16.507±0.082	16.209±0.100	0.206	
Sgr 1991	V4160 Sgr	NA	18:14:13.83	-32:12:28.5	—	—	—	—	—	—	—	ND
Sco 1992	V0992 Sco	NA	17:07:17.44	-43:15:22.0	17:07:17.45	-43:15:21.86	0.199	15.455±0.010	14.981±0.014	14.691±0.019	—	

Table 1. cont. Previously known novae in the VVV area.

Nova (Year)	Other Designation	Nova Type	RA [hh:mm:ss.ss]	DEC [dd:mm:ss.ss]	RA (VVV) [hh:mm:ss.ss]	DEC (VVV) [dd:mm:ss.ss]	Dist. ["]	<i>J</i> [mag]	<i>H</i> [mag]	<i>K_s</i> [mag]	<i>A_{K_s}</i> [mag]	Note
Sgr 1992a	V4157 Sgr	NA	18:09:34.90	-25:51:58.0	18:09:34.81	-25:51:56.55	1.900	15.820±0.045	15.355±0.053	15.095±0.057	0.238	MS:
Sgr 1992b	V4169 Sgr	NA	18:23:26.94	-28:21:59.7	—	—						ND
Sgr 1992c	V4171 Sgr	NA	18:23:41.34	-22:59:28.7	—	—						ND
Sgr 1993	V4327 Sgr	NA	18:12:49.82	-29:29:04.9	18:12:49.70	-29:29:04.38	1.613	16.960±0.085	16.560±0.112	16.352±0.136	0.100	:
Cru 1996	CP Cru	N+E	12:10:31.39	-61:45:09.5	12:10:31.36	-61:45:09.75	0.315	16.617±0.016	15.977±0.016	15.492±0.021	—	
Sco 1997	V1141 Sco	NA	17:54:11.33	-30:02:53.0	17:54:11.37	-30:02:51.51	1.600	16.272±0.136	15.943±0.192	15.739±0.204	0.258	MS:
Sco 1998	V1142 Sco	NA	17:55:24.99	-31:01:41.5	—	—						ND
Sgr 1998	V4633 Sgr	NA	18:21:40.49	-27:31:37.3	—	—						ND
Sgr 1999	V4444 Sgr	NA	18:07:36.20	-27:20:13.2	18:07:36.18	-27:20:13.92	0.787	16.323±0.094	15.690±0.091	15.406±0.089	0.211	
Sgr 2000	V4642 Sgr	NA	17:55:09.84	-19:46:01.0	17:55:09.89	-19:46:00.34	0.976	17.343±0.117	16.812±0.145	16.530±0.170	0.378	
Sco 2001	V1178 Sco	NA	17:57:06.98	-32:23:05.0	17:57:06.92	-32:23:05.32	0.801	14.838±0.019	14.112±0.016	13.788±0.017	0.261	MS
Sgr 2001	V4643 Sgr	NA	17:54:40.46	-26:14:15.2	17:54:40.47	-26:14:14.30	0.499	12.819±0.001	12.212±0.010	12.733±0.010	1.880	
Sgr 2001b	V4739 Sgr	NA	18:24:46.04	-30:00:41.1	18:24:46.11	-30:00:39.45	1.929	16.654±0.029	16.145±0.038	15.967±0.065	0.077	MS:
Sgr 2001c	V4740 Sgr	NA	18:11:45.82	-30:30:49.9	18:11:45.71	-30:30:50.14	1.377	18.103±0.239	17.615±0.257	17.126±0.249	0.101	MS:
Sgr 2002	V4741 Sgr	NA	17:59:59.63	-30:53:20.5	—	—						ND
Sgr 2002b	V4742 Sgr	NA	18:02:21.86	-25:20:32.2	—	—						ND
Sgr 2002d	V4744 Sgr	NA	17:47:21.74	-23:28:23.1	17:47:21.79	-23:28:24.49	1.544	17.066±0.140	16.259±0.129	16.083±0.150	0.313	MS:
Sgr 2003b	V5113 Sgr	NA	18:10:10.42	-27:45:35.2	—	—						ND
Oph 2004	V2574 Oph	NA	17:38:45.49	-23:28:18.5	17:38:45.52	-23:28:18.55	0.415	15.825±0.028	15.496±0.040	15.160±0.046	0.354	MS
Sco 2004	V1186 Sco	NA	17:12:51.21	-30:56:37.2	17:12:51.24	-30:56:37.56	0.509	14.622±0.010	14.242±0.013	13.912±0.015	0.218	
Sco 2004b	V1187 Sco	NA	17:29:18.81	-31:46:01.5	17:29:18.84	-31:46:01.35	0.363	14.545±0.010	14.047±0.013	13.708±0.018	0.727	
Sgr 2004	V5114 Sgr	NA	18:19:32.29	-28:36:35.7	18:19:32.38	-28:36:36.57	1.502	16.302±0.031	15.987±0.043	15.932±0.069	0.136	:
Cen 2005	V1047 Cen	N	13:20:49.74	-62:37:50.5	13:20:49.79	-62:37:50.63	0.387	14.373±0.010	13.664±0.010	12.841±0.010	—	
Nor 2005	V0382 Nor	NA	16:19:44.74	-51:34:53.1	16:19:44.79	-51:34:52.09	1.124	16.554±0.028	16.101±0.039	15.574±0.049	—	
Sco 2005	V1188 Sco	NA	17:44:21.59	-34:16:35.7	17:44:21.58	-34:16:33.87	1.836	17.239±0.174	16.589±0.180	16.441±0.193	0.322	MS:
Sgr 2005a	V5115 Sgr	NA	18:16:59.04	-25:56:38.8	—	—						ND
Sgr 2005b	V5116 Sgr	NA	18:17:50.77	-30:26:31.2	18:17:50.75	-30:26:31.86	0.708	17.535±0.088	16.263±0.050	16.163±0.081	0.084	
Oph 2006	V2575 Oph	N	17:33:13.06	-24:21:07.1	17:33:13.05	-24:21:07.05	0.132	17.117±0.072	16.520±0.091	15.998±0.098	0.488	
Sgr 2006	V5117 Sgr	NA	17:58:52.61	-36:47:35.1	17:58:52.57	-36:47:34.33	0.883	17.572±0.068	17.092±0.090	17.052±0.154	0.098	MS:
Oph 2007	V2615 Oph	NA	17:42:44.00	-23:40:35.1	17:42:44.00	-23:40:35.16	0.059	16.689±0.088	16.404±0.127	16.056±0.131	0.359	
Nor 2007	V0390 Nor	NA	16:32:11.51	-45:09:13.4	—	—						ND
Oph 2008a	V2670 Oph	NA	17:39:50.94	-23:50:01.0	17:39:50.92	-23:50:00.88	0.274	13.442±0.010	13.081±0.010	12.181±0.010	0.356	
Oph 2008b	V2671 Oph	N	17:33:29.67	-27:01:16.4	—	—						ND
Sgr 2008	V5579 Sgr	NA	18:05:58.88	-27:13:56.0	18:05:58.89	-27:13:55.91	0.129	14.490±0.018	13.873±0.018	12.541±0.010	0.237	
Sgr 2008b	V5580 Sgr	N	18:22:01.39	-28:02:39.8	18:22:01.48	-28:02:39.73	1.153	15.988±0.024	15.650±0.033	15.394±0.048	0.129	:
Oph 2009	V2672 Oph	NA	17:38:19.72	-26:44:13.7	—	—						ND
Sgr 2009a	V5581 Sgr	N:	17:44:08.44	-26:05:48.7	17:44:08.46	-26:05:47.78	0.948	11.448±0.010	11.445±0.010	10.687±0.010	0.595	ST
Sgr 2009b	V5582 Sgr	N	17:45:05.40	-20:03:21.5	17:45:05.42	-20:03:21.43	0.263	14.493±0.010	14.159±0.010	13.174±0.010	0.184	
Sgr 2009c	V5583 Sgr	NA	18:07:07.67	-33:46:33.9	18:07:07.68	-33:46:34.48	0.605	16.060±0.021	15.918±0.035	15.391±0.037	0.107	
Oph 2010	V2673 Oph	NA	17:39:40.90	-21:39:50.5	—	—						ND

Table 1. cont. Previously known novae in the VVV area.

Nova (Year)	Other Designation	Nova Type	RA [hh:mm:ss.ss]	DEC [dd:mm:ss.s]	RA (VVV) [hh:mm:ss.ss]	DEC (VVV) [dd:mm:ss.ss]	Dist. [']	<i>J</i> [mag]	<i>H</i> [mag]	<i>K_s</i> [mag]	<i>A_{K_s}</i>	Note
Oph 2010b	V2674 Oph	NA	17:26:32.19	-28:49:36.3	—	—	—	—	—	—	—	ND
Sgr 2010	V5585 Sgr	NA	18:07:26.95	-29:00:43.6	18:07:26.95	-29:00:43.59	0.016	11.921±0.010	11.906±0.010	11.250±0.010	0.170	
Sgr 2010b*	V5586 Sgr	N	17:53:03.00	-28:12:19.0	17:53:02.98	-28:12:18.84	0.339	7.764±0.010	—	10.609±0.010	0.724	ST
Sgr 2011	V5587 Sgr	NA	17:47:46.33	-23:35:13.1	—	—	—	—	—	—	—	ND
Sgr 2011b	V5588 Sgr	NA	18:10:21.35	-23:05:30.6	—	—	—	—	—	—	—	ND
Cen 2012b**	TCP J14250600-5845360	N:	14:25:06.00	-58:45:36.0	—	—	—	—	—	—	—	ND
Oph 2012b	PNV J17395600-2447420	N	17:39:56.00	-24:47:42.0	—	—	—	—	—	—	—	ND
Sco 2012	MOA 2012 BLG-320	NB:	17:50:53.90	-32:37:20.5	—	—	—	—	—	—	—	ND
Sgr 2012**	PNV J17452791-2305213	N:	17:45:28.03	-23:05:22.8	17:45:28.02	-23:05:22.72	0.125	15.813±0.035	15.421±0.047	15.178±0.056	0.274	
Sgr 2012c	PNV J17522579-2126215	NA	17:52:25.79	-21:26:21.5	—	—	—	—	—	—	—	ND
Sgr 2012d	PNV J18202726-2744263	N	18:20:27.26	-27:44:26.3	—	—	—	—	—	—	—	ND
	OGLE-2012-NOVA-01	N	17:56:49.39	-27:13:28.2	17:56:49.50	-27:13:28.59	1.518	17.439±0.12	17.440±0.366	17.018±0.455	0.726	:
	V1213 Cen	NA	13:31:15.80	-63:57:39.0	13:31:15.74	-63:57:38.41	0.717	13.855±0.01	13.664±0.010	12.803±0.010	—	MS
	PN G002.6+01.7	n:	17:45:08.60	-25:44:01.0	17:45:08.54	-25:44:01.99	1.288	14.888±0.02	13.859±0.022	13.465±0.024	0.531	:
	V0733 Sco	N:	17:39:42.88	-35:52:38.4	17:39:43.00	-35:52:38.62	1.523	14.505±0.01	13.667±0.010	13.370±0.011	0.416	:
	GR Sgr	NA:	18:22:58.50	-25:34:47.3	18:22:58.52	-25:34:47.28	0.217	15.071±0.01	14.693±0.017	14.506±0.023	0.143	
	AT Sgr	NA	18:03:30.87	-26:28:28.5	18:03:31.00	-26:28:28.74	1.815	17.218±0.17	16.923±0.271	16.325±0.225	0.432	MS:
	V2859 Sco	NA	17:50:36.09	-30:01:46.6	—	—	—	—	—	—	—	ND
	[KW2003] 105	n:	18:01:56.24	-27:22:55.6	18:01:56.25	-27:22:56.16	0.590	15.250±0.030	14.955±0.050	14.656±0.054	0.327	
	V0729 Sco	N:	17:22:02.66	-32:05:48.8	—	—	—	—	—	—	—	ND

Notes. * during eruption, ** nova progenitor

We defined as a valid match all cases where a source was found within 1 arcsec from the position given by the catalogue. This value is in agreement with the median values of the VVV image quality in the first season (0′89–0′87, respectively to J and K_s observations) and the typical astrometric accuracy of the photometric catalogues ($\lesssim 0′5$; Saito et al. 2012a). A complementary visual inspection of the images was performed for all novae candidates, in order to certify the presence (or absence) of a target in the given position. In some cases the source was rejected because of the presence of a faint object in a closer position to the coordinate, seen during the visual inspection of the images, but beyond the detection limit of the CASU aperture photometry, used to build the VVV photometric catalogues (see Section 2). In other cases multiple sources are seen in a similar close distance from the entry coordinates. In this procedure we secured the information for 55 novae within ≤ 1 arcsec from the catalogue position, being 27 of them within the VIRCAM pixel scale of $0′34 \text{ pixel}^{-1}$. A complementary search included also objects matching the position given by the catalogue within 2 arcsec. By this procedure we retrieved the photometry of another 37 objects. These are all fainter than $K_s \sim 13$ mag and were classified as doubtful sources. We note that due to the source confusion in the most crowded regions of Galactic plane and bulge, a search based only on the coordinates does not guarantee that in all cases the source found in a closer position to the coordinates is in fact the nova remnant. Thus these should be seen as candidate near-IR counterparts for the novae remnant.

Therefore, from the 140 novae within the VVV area, we are able to provide the JHK_s colours of 93 objects: 55 classified as valid matches (27 within the pixel scale), and 37 as doubtful sources. The other objects are beyond our detection limit (progenitors in quiescence with $K_s \gtrsim 18$ mag), or with coordinates not sufficiently accurate to allow us to identify the target in the field. Table 1 presents the JHK_s photometry of all novae detected in the VVV area while in the Appendix we provide the composite JHK_s finding charts for all objects.

Since the VVV JHK_s observations were performed during 2010–2011, we are also able to provide the information about the progenitors of the most recent novae, as well as the fading curve after the nova eruption (see Section 5). Interestingly, the observations of Nova Sgr 2010b were secured while the object was in eruption (Saito & Minniti 2012a). Complementary information, including the timings of the VVV colour and variability campaign observations for all novae erupted in this century, is presented in Table 3.

4. The near-IR Colours

Figure 3 shows in the top panels the K_s vs. $(J - K_s)$ colour-magnitude diagram (CMD) and the $(J - H)$ vs. $(H - K_s)$ colour-colour diagram (CCD) for all novae in the VVV area. We used different symbols to denote the objects classified as valid matches and the doubtful ones, as described in the previous Section. The reddening vector associated with an extinction of $E(B - V) = 1$, based on the relative extinctions of the VISTA filters, and assuming the Cardelli et al. (1989) extinction law, is also shown.

The Galactic novae range in magnitude and colour, with all objects appearing red, with $(J - K_s) > 0$ (the only exception is Nova Cir 1906, with $(J - K_s) = -0.228$). Interestingly, a large fraction of novae are beyond detection in previous near-IR surveys (e.g., 2MASS, DENIS; Skrutskie et al. 2006; Epchtein et al. 1994), thus we are now reporting their IR-colours for the first time in an homogeneous data set. We note that the novae are

spread across the whole VVV area (see Fig. 1), and therefore are affected by different extinction. For instance, in the bulge area where most novae are located, reddening spans from $E(B - V) \lesssim 0.2$ at $b \sim -10^\circ$ to $E(B - V) \sim 10$ closer to the Galactic centre (e.g., Gonzalez et al. 2012).

In the $(J - H)$ vs. $(H - K_s)$ CCD the objects are seen more concentrated at low values of $(H - K_s)$, but spread along $(J - H)$ by more than 1 mag. The colours of main sequence stars (with spectral type from B0 to M4, adapted from Ducati et al. 2001) are presented in the CMD in the case of $A_{K_s} = 0$ mag (no extinction) and applying the median value of extinction among our targets of $A_{K_s} = 0.243$ mag (corresponding to $E(B - V) \sim 0.67$ mag). The comparison reveals that part of our sources coincide in colour with the main sequence stars and therefore suggests that some of our novae candidates can be actually old field stars, which match a position close to the novae coordinates, and suffer from reddening at different levels. Individual values of A_{K_s} for all bulge novae are listed in Table 1. Although the Ducati et al. (2001) data are in the JHK system, it is sufficiently close to the VISTA system that is useful for the comparison. Four objects are seen with the most extreme colours: Nova Sgr 2001 and Nova Sgr 2005b, with the largest $(J - H)$ but low $(H - K_s)$; and Nova Sgr 2008 and Nova Sgr 2009b, showing the largest $(H - K_s)$ values at relatively low values of $(J - H)$. The complementary JHK_s spectral energy distributions (SED) for these selected objects are shown in Fig. 4. While Nova Sgr 2001 and Nova Sgr 2005b show a maximum close to the H -band, the SED of Nova Sgr 2008 and Nova Sgr 2009b reveal a monotonic increase in flux towards longer wavelengths.

In order to minimize the reddening effects we calculated the dereddened J_0 , H_0 , and K_{s0} colours for the bulge novae, using the maps of Gonzalez et al. (2012), the relative extinctions of the VISTA filters, and assuming the Cardelli et al. (1989) extinction law. A dereddened K_{s0} vs. $(J - K_s)_0$ CMD is presented in the bottom-left panel of Fig. 3. Since the Gonzalez et al. (2012) maps do not cover the disk area we prefer to exclude from the plot the few novae located in this region, instead of using a different prescription for the extinction in the disk, which does not guarantee a good agreement with the procedure used in the bulge area (e.g., Saito et al. 2012a). We also note that the reddening law is known to change close to in the Galactic center (e.g., Nishiyama et al. 2009), but in our sample just one object (Nova Sgr 2001) belongs to this region.

A set of reddening-free indices provided by Catelan et al. (2011), based on the extinction law of Rieke & Lebofsky (1985) for the VISTA filters was also computed. The m_4 pseudo-magnitude and the c_3 pseudo-colour are defined as

$$m_4 \equiv K_s - 1.22(J - H), \quad (1)$$

$$c_3 \equiv (J - H) - 1.47(H - K_s). \quad (2)$$

The m_4 vs. c_3 CMD is shown in the bottom-right panel of Fig. 3. We note the indices shown in the equations depend on the effective wavelengths of each filter, assumed to be a flat distribution here, which is certainly different from the near-IR spectra of novae. Refined indices based on actual near-IR spectra covering different luminosity classes and spectral types are currently being computed, and quantitative tests in the case of actual near-IR spectra of novae will also be carried out in the future.

One important aspect seen in all panels of Fig. 3 is the absence of a clear-cut correlations or trends, even using dereddened

Table 2. Novae eruptions in the VVV area from January 2001 to the December 2012. More detailed information are provided for the 2010-2012 novae.

Nova	Other Designation	Eruption Date	VVV JHK_s Observation	First K_s -band epoch (variability campaign)	Note
Sco 2001	V1178 Sco	2001	2010 08 10	2010 09 12	Remnant
Sgr 2001	V4643 Sgr	2001	2010 04 09	2011 08 06	Remnant
Sgr 2001b	V4739 Sgr	2001	2010 08 14	2010 10 15	Remnant
Sgr 2001c	V4740 Sgr	2001	2010 08 15	2011 08 05	Remnant
Sgr 2002	V4741 Sgr	2002	2010 08 10	2010 09 12	Remnant
Sgr 2002b	V4742 Sgr	2002	2010 03 28	2010 03 30	Remnant
Sgr 2002d	V4744 Sgr	2002	2010 03 18	2010 09 29	Remnant
Sgr 2003b	V5113 Sgr	2003	2010 03 28	2010 08 26	Remnant
Oph 2004	V2574 Oph	2004	2010 03 30	2010 04 10	Remnant
Sco 2004	V1186 Sco	2004	2010 08 03	2010 08 26	Remnant
Sco 2004b	V1187 Sco	2004	2010 08 03	2010 08 26	Remnant
Sgr 2004	V5114 Sgr	2004	2010 08 15	2010 10 24	Remnant
Cen 2005	V1047 Cen	2005	2010 03 07	2010 03 29	Remnant
Nor 2005	V0382 Nor	2005	2010 03 06	2010 03 06	Remnant
Sco 2005	V1188 Sco	2005	2010 10 01	2011 07 27	Remnant
Sgr 2005a	V5115 Sgr	2005	2010 03 28	2010 03 30	Remnant
Sgr 2005b	V5116 Sgr	2005	2010 08 15	2010 10 15	Remnant
Oph 2006	V2575 Oph	2006	2010 03 30	2010 04 09	Remnant
Sgr 2006	V5117 Sgr	2006	2010 04 23	2010 10 25	Remnant
Oph 2007	V2615 Oph	2007	2010 03 17	2011 06 12	Remnant
Nor 2007	V0390 Nor	2007	2010 03 16	2010 08 15	Remnant
Oph 2008a	V2670 Oph	2008	2010 03 17	2011 06 12	Remnant
Oph 2008b	V2671 Oph	2008	2011 05 07	2011 06 13	Remnant
Sgr 2008	V5579 Sgr	2008	2010 04 12	2011 08 05	Remnant
Sgr 2008b	V5580 Sgr	2008	2010 04 08	2010 08 27	Remnant
Oph 2009	V2672 Oph	2009	2010 04 13	2011 06 13	Remnant
Sgr 2009a	V5581 Sgr	2009	2010 03 30	2010 03 30	Remnant
Sgr 2009b	V5582 Sgr	2009	2010 04 10	2011 06 14	Remnant
Sgr 2009c	V5583 Sgr	2009	2010 04 23	2010 08 18	Remnant
Oph 2010	V2673 Oph	2010 01 15 ^a	2010 04 10	2011 06 14	Remnant
Sgr 2010	V5585 Sgr	2010 01 20 ^b	2010 04 23	2010 08 26	Remnant
Oph 2010b	V2674 Oph	2010 02 18 ^c	2011 05 09	2011 07 26	Remnant
Sgr 2010b	V5586 Sgr	2010 04 23.782 ^d	2010 04 23.2457 (<i>H</i>) 2010 04 23.2479 (K_s) 2010 04 23.2501 (<i>J</i>)	2010 09 12	During eruption
Sgr 2011	V5587 Sgr	2011 01 25 ^e	2010 03 18	2010 09 29	Progenitor
Sgr 2011b	V5588 Sgr	2011 04 07 ^f	2010 04 21	2010 10 06	Progenitor
Cen 2012b	TCP J14250600-5845360	2012 04 05 ^g	2010 03 27	2010 03 09	Progenitor
Sgr 2012	PNV J17452791-2305213	2012 04 21 ^h	2010 03 18	2010 09 29	Progenitor
Oph 2012b	PNV J17395600-2447420	2012 05 19 ⁱ	2010 04 13	2011 06 12	Progenitor
Sco 2012	MOA 2012 BLG-320	2012 05 22 ^j	2010 08 29	2010 09 25	Progenitor
Sgr 2012c	PNV J17522579-2126215	2012 06 26 ^k	2010 03 25	2010 09 29	Progenitor
Sgr 2012d	PNV J18202726-2744263	2012 07 12 ^l	2010 04 08	2010 08 27	Progenitor
	OGLE-2012-NOVA-01	2012 05 02 ^m	2010 03 28	2010 08 26	Progenitor

References. ^a Nakano et al. (2010a), ^b Nishiyama et al. (2010), ^c Nakano et al. (2010b), ^d Kiyota et al. (2010), ^e Nakano et al. (2011), ^f Nishiyama et al. (2011), ^g Green (2012a), ^h Green (2012b), ⁱ Walter & Buil (2012), ^j Waagen (2012), ^k Yamaoka & Itagaki (2012), ^l Nishimura & Nakano (2012), and ^m Kozłowski et al. (2012).

colours and reddening-free indices, the resulting distributions do not appear to have straightforward interpretations. The differences in colour arise mostly because (i) the objects are seen at different distances and positions in the Galaxy, and thus can suffer from extinction and reddening at different levels, compared to the 2D reddening maps of (Gonzalez et al. 2012) and (ii) the

spectral energy distribution in the near-IR can be affected by emission lines and thermal emission by a dust shell produced during eruption. The latter are time-dependent and valid mostly for recent novae. Depending on the evolution of the dust shells created in the outbursts, a variety of emission lines are seen in early post-outburst near-IR spectra. Moreover, for older novae

the peak emission from the dust shells is shifted to longer wavelengths (e.g., Venturini et al. 2002; Banerjee & Ashok 2012).

Four objects seen with the extreme colours on the plots of Fig. 3 are discussed in more detail in the following, namely Nova Sgr 2001, Nova Sgr 2005b, Nova Sgr 2008 and Nova Sgr 2009b.

Ashok et al. (2006) classified Nova Sgr 2001 as a “NA” fast novae, with absence of dust formation after the eruption. Its near-IR spectrum evolves significantly from the early decline stage (March 2001) to the coronal phase (August 2001, Ashok et al. 2006). Nova Sgr 2001 is the innermost known nova in the Galaxy, with coordinates $(l, b) = (3.345, -0.337)$ deg, with an extinction of $A_{K_s} = 1.88$ mag according to the maps of Gonzalez et al. (2012) using Nishiyama et al. (2009) extinction law, equivalent to $A_V \approx 15.9$ mag.

Our data taken during the quiescent phase (on April 2010) show the remnant of Nova Sgr 2001 as a relatively blue object, with the maximum intensity in the near-IR around the H -band (see Fig. 4). However, data taken with UKIRT on March 2012 show Nova Sgr 2001 with a flatter SED in the near-IR, with the maximum intensity towards longer wavelengths (Varricatt et al. 2012).

Ashok et al. (2006) estimated a distance to the object of $d = 3.3$ kpc. Thus, since our calculations using Gonzalez et al. (2012) maps assume the total extinction in the line of sight, it could not be a good approach to estimate the reddening for nearby objects, overestimating the corrections. In this case, three-dimensional extinction maps are necessary, in order to estimate the relative extinction at given distance (e.g., Chen et al. 2013). On the other hand, the c_3 colour seems to be dominated by the H -band (by construction, see Equation 2), thus the presence of features such as emission lines or simply the slope of the SED contribute to shift the value of the c_3 pseudo-color from a relatively small to a relatively large value, depending on whether the emission peaks around the H -band or not. This explains why Nova Sgr 2001 and Nova Sgr 2005b, whose spectra do peak around H (Fig. 4), have large *positive* c_3 values, whereas the remaining novae, whose spectra monotonically increase towards longer wavelengths, have – on the contrary – large *negative* c_3 values.

Nova Sgr 2005b is similar in color with Nova Sgr 2001. Its remnant is a Supersoft X-ray variable source, presenting an orbital period of $P_{orb} = 2.97$ hr (Dobrotka et al. 2008; Sala et al. 2008, 2010), which puts the object on the edge of the 2 – 3 hr CVs period gap (e.g., Warner 2003). The object is located beyond the bulge, with $(l, b) = (2.136, -6.832)$ deg and a distance of $d = 11 \pm 3$ kpc estimated by Sala et al. (2008). Nova Sgr 2005b lies in the lower part of the CMDs, with $K_s = 16.163$ and $K_{s,0} = 16.079$. The presence of such distant objects in our data demonstrates our capability to monitor even the most distant novae in the Galaxy.

In the other extreme are Nova Sgr 2008 and 2009b. Nova Sgr 2008 was discovered in eruption on 2008 April 18 (Nakano et al. 2008). It is a nearby fast Fe II nova, located at $(l, b) = (3.734, -3.022)$ deg at distance of $d = 4.4 \pm 0.2$ kpc (Russell et al. 2008; Raj et al. 2011). The very red colors even in $(J - K_s)_0$ are related to the presence of dust. Spectra taken in the late stages after the eruption indicate dust formation during the nova remnant’s development (Raj et al. 2011). Nova Sgr 2009b (Sun & Gao 2009) is located in a low-extinction region with $(l, b) = (7.531, 4.719)$ deg and $A_{K_s} = 0.1845$ mag. There are no entries in the literature estimating its distance or classifying the nova remnant. However, by comparing their colours, one can infer that Nova Sgr 2009b was similar to the Nova Sgr 2008

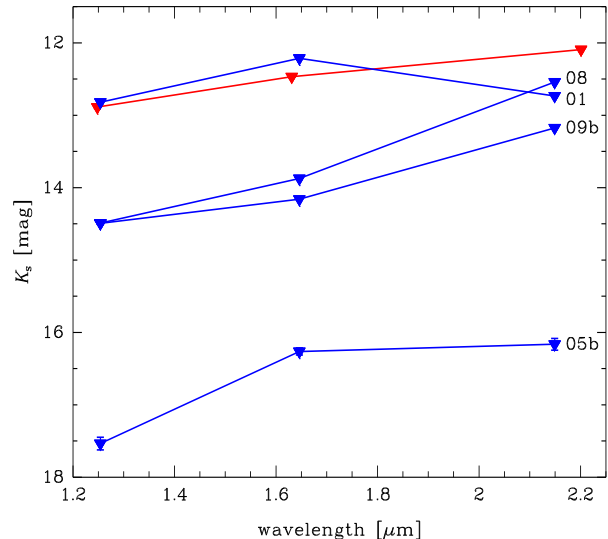


Fig. 4. Spectral energy distribution for the novae showing the extreme colours in Fig. 3: Nova Sgr 2001, Nova Sgr 2005b, Nova Sgr 2008, and Nova Sgr 2009b. Data for Nova Sgr 2001 taken with UKIRT are also shown (red points; see Section 4).

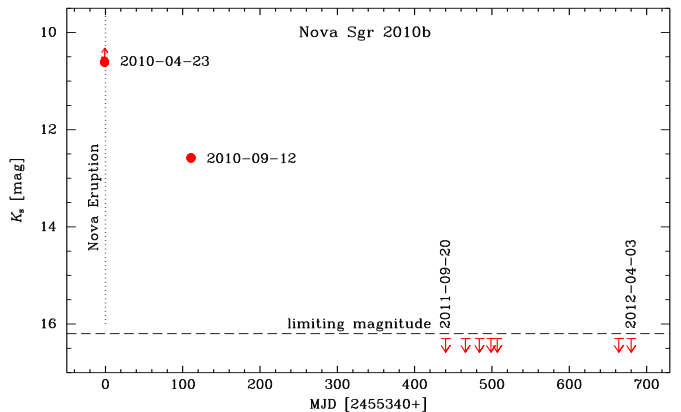


Fig. 6. VVV K_s -band light curve of Nova Sgr 2010b. The VVV data caught the object about 0.5 days before its first detection in eruption. The object is seen as a saturated source on 23 March 2010 and recorded about 2 mags fainter on 12 Sep 2010. Sgr 2010b is beyond detection ($K_s \geq 16.2$ mag in the VVV K_s -band aperture catalogues for this field) in a sequence of observations from Sep 2011 to Apr 2012.

remnant. In this case, Nova Sgr 2009b could be surrounded by dust, expelled from the system after the eruption.

5. The VVV variability campaign on Novae

The IR photometric monitoring of several novae outbursts has allowed already in the 1990’s to distinguish between two fundamentally different types of objects, usually referred to as CO and ONe novae. While the first seems to arise from thermonuclear runaway on a relatively low-mass WD and tends to form considerable amounts of dust at later stages, the latter turn out to be associated with massive ($\geq 1.2 M_{\odot}$) WD that have outbursts which exhibit a coronal line emission phase with little or no dust production.

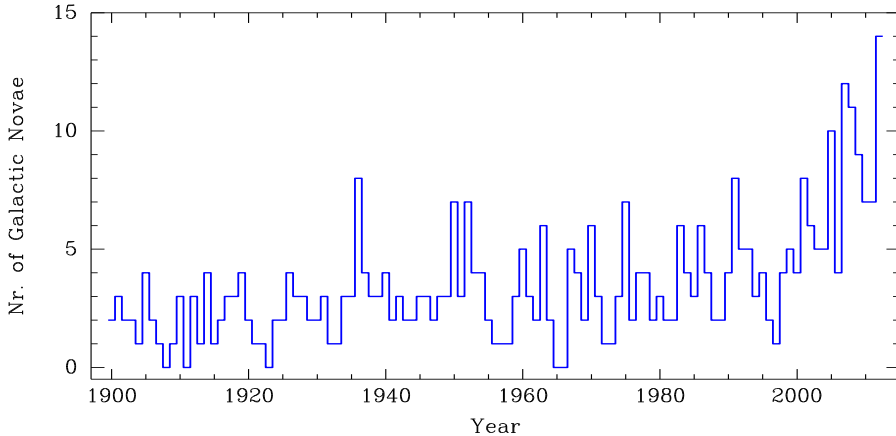


Fig. 5. Historical record of all classical novae discovered in the MW since year 1900. Despite the increment in the nova rate seen in the last two decades, the nova rate is still below that seen in nearby galaxies. The data are completed as of December 2012.

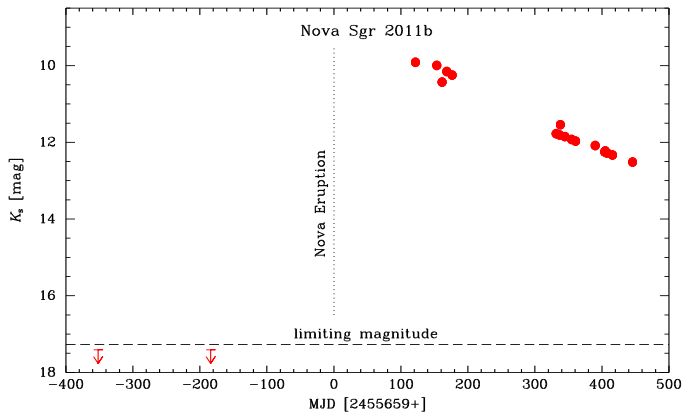


Fig. 7. VVV K_s -band light curve of Nova Sgr 2011b. Several epochs starting on 21 Apr 2011 registered the object fading after its eruption on 07 Apr 2011. The Nova progenitor is beyond the limiting magnitude in two observations taken during 2010 ($K_s \gtrsim 17.3$ mag).

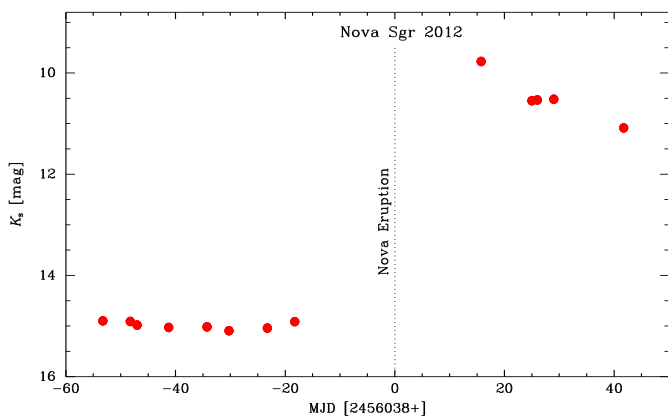


Fig. 8. VVV K_s -band light curve of Nova Sgr 2012. Its eruption was detected on 21 Apr 2012. The Nova progenitor is seen at $K_s \sim 15.0$ mag in five observations earlier in 2012, while a few observations starting about a hundred days after the eruption registered its fading curve.

Particularly useful in identifying extreme CO and ONe novae are the K_s -band light curves: because of the thermal emission from dust during the condensation phase, CO Novae reach an emission peak within a few months from the optical maximum, declining exponentially thereafter as consequence of the decreasing density of the shell owing to expansion (emblematic is the case of NQ Vul; Sato et al. 1978). ONe novae, on the contrary, decline rapidly shortly after the optical maximum and then have a positive change in the slope rate (e.g., V1974 Cyg; Woodward et al. 1997) because of the increasing contribution of several IR forbidden emission lines (e.g., [Ca VIII] $2.32 \mu\text{m}$, [Si VII] $2.47 \mu\text{m}$), whose intensity strengthens during the coronal phase acting thus as effective coolant of the ejecta (e.g., as in QU Vul; Greenhouse et al. 1988).

The VVV Survey, for the first time, will provide well-sampled light curves in the K_s -band for about 100 Galactic novae that exploded in the last ~ 150 years in the Galactic bulge and in the southern part of the Galactic disk. At the time of writing, the VVV variability campaign is ongoing, and in the next few years until the completion of the survey (2016 or later), we would be able to finally build a coherent picture of nova IR behavior, at quiescence, as well as to discover new novae in highly-extincted regions that are missed in the optical.

There are about 400 known novae in the Milky Way, but the comparison with the nova rate in nearby galaxies shows that a number of novae are lost every year in the Galaxy. While the historical records show a rate below a dozen nova discovered per year in the MW (see Fig. 5), several results point to a nova rate spanning between $\sim 30 - 40 \text{ yr}^{-1}$, or even higher reaching up to $\sim 260 \text{ yr}^{-1}$ (Liller & Mayer 1987; Liller 1993; della Valle & Livio 1994; Shafter 1997; Shafter & Irby 2001).

Not coincidentally, the spatial distribution of novae in the bulge and southern plane shows a “zone of avoidance”(see Fig. 1), with just a few objects belonging to the high-extinction regions of the Galaxy. This arises because the current searches for novae are performed with small-aperture telescopes in the optical. The VVV Survey combines deep and high-spatial resolution observations in the near-infrared, allowing one to search for novae even in the most crowded and high extinction regions of our Galaxy. Very illustrative is the recent discovery of VVV-NOV-001, the first Nova candidate from the VVV data, located in a high extinction region in the inner bulge with

$(l, b) = (8.897, -0.158)$ deg and $A_V \sim 11$ mag (Saito et al. 2012c).

Fig. 2 shows the magnitude range covered by VVV at different levels of crowding in the bulge. Even in the most problematic case which is close to the Galactic center, the VVV observations allow us to monitor over a range in magnitudes spanning from $\Delta K_s > 7$ mag, reaching even $\Delta K_s \sim 10$ mag when using data taken below $5\text{-}\sigma$ accuracy and saturated sources. As of this writing, we are able to provide light curves with a few points for some objects, which demonstrates our capability to monitor novae at all phases depending on the magnitude in each case. Figs. 6, 7 and 8 show VVV light curves of Nova Sgr 2010b (Saito & Minniti 2012a), 2011 and 2012 (Saito & Minniti 2012b), respectively.

These K_s -band light curves at quiescence will allow us to study any kind of orbital effects which could be related to the influence on the secondary star by the accreting WD, and when combined with the IR colors will also help quantify (via modeling of ellipsoidal variations of the secondary) fundamental parameters of the nova system, such as spectral type of the secondary, mass ratios, orbital periods and inclinations (Mason et al. 1998).

6. Perspectives on the search for novae using the VVV images

There is a well-known discrepancy on the actual amount of mass ejected in a CN outburst as predicted by theory and numerical simulations on one side, and as derived from infrared and radio observations on the other side - being the latter systematically higher by up to a factor ~ 10 (Shaviv 2002; Shaviv & Dotan 2012).

Even if there are strong caveats on the methods and assumptions used for determining the mass of the ejecta (e.g., Shara et al. 2010), the analysis of the most recent observational material seems in fact to suggest for the ejecta of classical novae a lower mass and higher velocities ($10^{-4} - 10^{-5}M_\odot$ and up to 6000 km s^{-1} , respectively, as in the extreme case of LMC1991 – Schwarz et al. 2001) than thought before. Identifying where such a discrepancy stems from would have dramatic consequences on our understanding of the nova phenomenon, e.g., by clarifying its role in the chemical evolution of the galaxy.

By supposing expansion velocities of the nova remnants larger than 1000 km s^{-1} , it is reasonable to expect that at least the closest/fastest novae produce nebular remnants that eventually may be spatially resolved even from ground-based telescopes. Imaging such remnants allows the investigation of fundamental correlations between the properties of the central binary, the evolution of the outburst and the ejecta shaping mechanism, and also provides a direct measure of the distance to the nova by combining the angular expansion rate with spectroscopically derived expansion velocities, i.e., the so-called *expansion parallax method* (Baade 1940; Martin 1989).

While the infrared imagery has several advantages over the optical one (e.g., the extinction – which is often poorly known for novae – is conveniently reduced), up to now only a handful of nova remnants have been searched (and even fewer spatially resolved) in this spectral region, compared to more than 40 nova remnants resolved in the optical and ~ 10 in the radio.

Thanks to the large sky area covered and to the higher spatial resolution than previous IR surveys (such as 2MASS and DENIS), VVV is in unique position to perform for the first time a systematic search for remnants of classical novae that exploded

in the last decades within the inner, highly-extincted regions of the MW. Even assuming a representative distance to a nova of 4 kpc (about half-way to the Galactic center) and a very conservative expansion velocity of 1000 km s^{-1} , VVV is in fact potentially able to spatially resolve the corresponding nebular remnants after ~ 40 years from the outburst, taking into account the VIRCAM pixel scale ($0''.34 \text{ pixel}^{-1}$) and a nebula angular size of $2''$. No resolved novae shells have yet been detected in the VVV imaging data. In a forthcoming phase of the survey a search for novae using imaging will be conducted on the deep, stacked K_s -band images, using more focused image analysis such as point spread function (PSF) subtraction or difference image analysis (DIA, e.g., Saito et al. 2012a).

7. Conclusions

We presented a near-IR catalogue of novae within the VVV area covering the MW bulge and southern Galactic plane area. From the 140 objects found in the VSX/AAVSO catalogue, we reported the JHK_s colours of 93 objects. The rest were beyond detection or heavily blended sources. Colour-magnitude and colour-colour diagrams were presented, as well as CMDs using dereddened colours and reddening-free indices. These should be used with caution since in the case of nearby objects the dereddened colours can overestimate the corrections, by assuming the total extinction in the line of sight. Likewise, reddening-free near-IR indices specifically devised for the study of novae would also be of considerable interest, given their different spectral shapes compared with those typically assumed in the computation of these indices.

Thanks to its higher spatial resolution in the near-IR, and large K_s -range covered by the observations, the VVV survey can be a major contributor for the search and study of novae in the Galaxy, mainly in the most crowded and high-extinction regions of the MW, beyond the capabilities of the current searches for novae in optical wavelengths.

VVV can produce well-sampled light curves covering many years for Galactic novae belonging both to the bulge and the southern part of the disk, even for objects during or fading after eruption. The recent report of VVV-NOV-001, the first nova candidate from the VVV data discovered in the inner bulge, is an illustrative example. Surely, the first of many more to come. The possibility to search for novae using the VVV imaging is accordingly a very promising path to unveiling the heretofore hidden population of heavily obscured novae.

Acknowledgements. We gratefully acknowledge use of data from the ESO Public Survey programme ID 179.B-2002 taken with the VISTA telescope, data products from the Cambridge Astronomical Survey Unit, and funding from the FONDAF Center for Astrophysics 15010003, the BASAL CATA Center for Astrophysics and Associated Technologies PFB-06, the FONDECYT from CONICYT, and the Ministry for the Economy, Development, and Tourism's Programa Iniciativa Científica Milenio through grant P07-021-F, awarded to The Milky Way Millennium Nucleus. Support for R.A. is provided by Proyecto GEMINI CONICYT 32100022 and via a Postdoctoral Fellowship by the School of Engineering at Pontificia Universidad Católica de Chile. M.C. and I.D. acknowledge funding from Proyecto FONDECYT Regular 1110326. J.B. acknowledges funding from Proyecto FONDECYT Regular 1120601. R.K. acknowledges partial support from FONDECYT through grant n. 1130140. This research has made use of the International Variable Star Index (VSX) database, operated at AAVSO, Cambridge, Massachusetts, USA.

References

Ashok, N. M., Banerjee, D. P. K., Varricatt, W. P., & Kamath, U. S. 2006, MNRAS, 368, 592

Baade, W. 1940, *PASP*, 52, 386
 Banerjee, D. P. K., & Ashok, N. M. 2012, *Bulletin of the Astronomical Society of India*, 40, 243
 Cardelli, J. A., Clayton, G. C., & Mathis, J. S. 1989, *ApJ*, 345, 245
 Catelan, M., Minniti, D., Lucas, P. W., et al. 2011, *RR Lyrae Stars, Metal-Poor Stars, and the Galaxy*, 145
 Chen, B. Q., Schultheis, M., Jiang, B. W., et al. 2013, *A&A*, 550, A42
 Darnley, M. J., Bode, M. F., Kerins, E., et al. 2004, *MNRAS*, 353, 571
 Darnley, M. J., Bode, M. F., Kerins, E., et al. 2006, *MNRAS*, 369, 257
 della Valle, M., & Livio, M. 1994, *A&A*, 286, 786
 della Valle, M., & Livio, M. 1998, *ApJ*, 506, 818
 Dobrotka, A., Retter, A., & Liu, A. 2008, *A&A*, 478, 815
 Ducati, J. R., Bevilacqua, C. M., Rembold, S. B., & Ribeiro, D. 2001, *ApJ*, 558, 309
 Epchtein, N., de Batz, B., Copet, E., et al. 1994, *Ap&SS*, 217, 3
 Frank, J., King, A., & Raine, D. J. 2002, *Accretion Power in Astrophysics*, by Juhan Frank and Andrew King and Derek Raine, pp. 398. ISBN 0521620538. Cambridge, UK: Cambridge University Press, February 2002.,
 Gaposchkin, C. H. P. 1957, Amsterdam, North-Holland Pub. Co.; New York, Interscience Publishers, 1957.,
 Green, D. W. E. 2012, *Central Bureau Electronic Telegrams*, 3073, 1
 Green, D. W. E. 2012, *Central Bureau Electronic Telegrams*, 3089, 1
 Greenhouse, M. A., Grasdalen, G. L., Hayward, T. L., Gehrz, R. D., & Jones, T. J. 1988, *AJ*, 95, 172
 Gonzalez, O. A., Rejkuba, M., Zoccali, M., et al. 2012, *A&A*, 543, A13
 Liller, W., & Mayer, B. 1987, *PASP*, 99, 606
 Liller, W. 1993, *Rev. Mexicana Astron. Astrofis.*, 26, 41
 Martin, P. G. 1989, *Classical Novae*, 73
 Mason, C. G., Gehrz, R. D., Woodward, C. E., et al. 1998, *ApJ*, 494, 783
 Minniti, D., Lucas, P. W., Emerson, J. P., et al. 2010, *New A*, 15, 433
 Nakano, S., Nishiyama, K., & Kabashima, F. 2008, *Central Bureau Electronic Telegrams*, 1342, 1
 Nakano, S., Nishimura, H., Itagaki, K., et al. 2010, *IAU Circ.*, 9111, 2
 Nakano, S., Nishimura, H., Kiyota, S., et al. 2010, *IAU Circ.*, 9119, 1
 Nakano, S., Nishimura, H., Kiyota, S., & Yusa, T. 2011, *IAU Circ.*, 9196, 1
 Nishimura, H., & Nakano, S. 2012, *Central Bureau Electronic Telegrams*, 3166, 1
 Nishiyama, S., Tamura, M., Hatano, H., et al. 2009, *ApJ*, 696, 1407
 Nishiyama, K., Kabashima, F., Liller, W., Yusa, T., & Maehara, H. 2010, *IAU Circ.*, 9140, 1
 Nishiyama, K., Kabashima, F., Maehara, H., & Kiyota, S. 2011, *IAU Circ.*, 9203, 1
 Kiyota, S., Vollmann, W., Koberger, H., et al. 2010, *IAU Circ.*, 9112, 1
 Kozłowski, S., Poleski, R., Udalski, A., et al. 2012, *The Astronomer's Telegram*, 4323, 1
 Raj, A., Ashok, N. M., & Banerjee, D. P. K. 2011, *MNRAS*, 415, 3455
 Rieke, G. H., & Lebofsky, M. J. 1985, *ApJ*, 288, 618
 Russell, R. W., Rudy, R. J., Lynch, D. K., et al. 2008, *IAU Circ.*, 8948, 1
 Saito, R. K., Hempel, M., Minniti, D., et al. 2012, *A&A*, 537, A107
 Saito, R. K., Minniti, D., Dias, B., et al. 2012, *A&A*, 544, A147
 Saito, R. K., Minniti, D., Angeloni, R., & Catelan, M. 2012, *The Astronomer's Telegram*, 4426, 1
 Saito, R. K., & Minniti, D. 2012, *The Astronomer's Telegram*, 4353, 1
 Saito, R. K., & Minniti, D. 2012, *The Astronomer's Telegram*, 4372, 1
 Sala, G., Hernanz, M., Ferri, C., & Greiner, J. 2008, *ApJ*, 675, L93
 Sala, G., Hernanz, M., Ferri, C., & Greiner, J. 2010, *Astronomische Nachrichten*, 331, 201
 Sato, S., Kawara, K., Kobayashi, Y., et al. 1978, *PASJ*, 30, 419
 Schwarz, G. J., Shore, S. N., Starrfield, S., et al. 2001, *MNRAS*, 320, 103
 Shafter, A. W. 1997, *ApJ*, 487, 226
 Shafter, A. W., & Irby, B. K. 2001, *ApJ*, 563, 749
 Shafter, A. W., Bode, M. F., Darnley, M. J., et al. 2011, *ApJ*, 727, 50
 Shara, M. M., Yaron, O., Prialnik, D., & Kovetz, A. 2010, *ApJ*, 712, L143
 Shaviv, N. J. 2002, *Classical Nova Explosions*, 637, 259
 Shaviv, N. J., & Dotan, C. 2012, *Mem. Soc. Astron. Italiana*, 83, 792
 Skrutskie, M. F., et al. 2006, *AJ*, 131, 1163
 Sun, G., & Gao, X. 2009, *IAU Circ.*, 9049, 1
 Udalski, A., Szymanski, M., Kaluzny, J., Kubiak, M., & Mateo, M. 1993, *Acta Astron.*, 43, 69
 Varricatt, W. P., Banerjee, D. P. K., & Ashok, N. M. 2012, *The Astronomer's Telegram*, 4405, 1
 Venturini, C. C., Rudy, R. J., Lynch, D. K., Mazuk, S., & Puetter, R. C. 2002, *AJ*, 124, 3009
 Waagen, E. O. 2012, *AAVSO Alert Notice*, 461, 1
 Walter, F. M., & Buil, C. 2012, *Central Bureau Electronic Telegrams*, 3124, 1
 Warner, B. 2003, *Cataclysmic Variable Stars*, by Brian Warner, pp. 592. ISBN 052154209X. Cambridge, UK: Cambridge University Press, September 2003.,
 Williams, R. E. 1992, *AJ*, 104, 725
 Woodward, C. E., Gehrz, R. D., Jones, T. J., Lawrence, G. F., & Skrutskie, M. F. 1997, *ApJ*, 477, 817
 Yamaoka, H., & Itagaki, K. 2012, *Central Bureau Electronic Telegrams*, 3156, 1

Appendix A: VVV Novae finding charts

In this section we present the finding charts for all Novae in the VVV Survey area, listed in Table 1. In most cases the charts are JHK_s composite images, unless when explicitly marked as a K_s -band image. All charts are $30'' \times 30''$ in size, oriented in Galactic coordinates, with the positive Galactic longitude pointing up. A cross marks the coordinates given by the catalogue and helps one to check the notes we adopted in Table 1.



Fig. A.1. First row: Nova Sgr 1893, Nova Sgr 1897, Nova Sgr 1899 and Nova Sco 1901. Second row: Nova Sgr 1901, Nova Sgr 1905, Nova Cir 1906 and Nova Sco 1906. Third row: Nova Sgr 1910, Nova Sgr 1914c, Nova Sgr 1917 and Nova Sgr 1919. Fourth row: Nova Sco 1922, Nova Sgr 1924, Nova Sgr 1926, Nova Sgr 1926a. Last row: Nova Sco 1928, Nova Sgr 1928, Nova Sgr 1930 and Nova Cen 1931

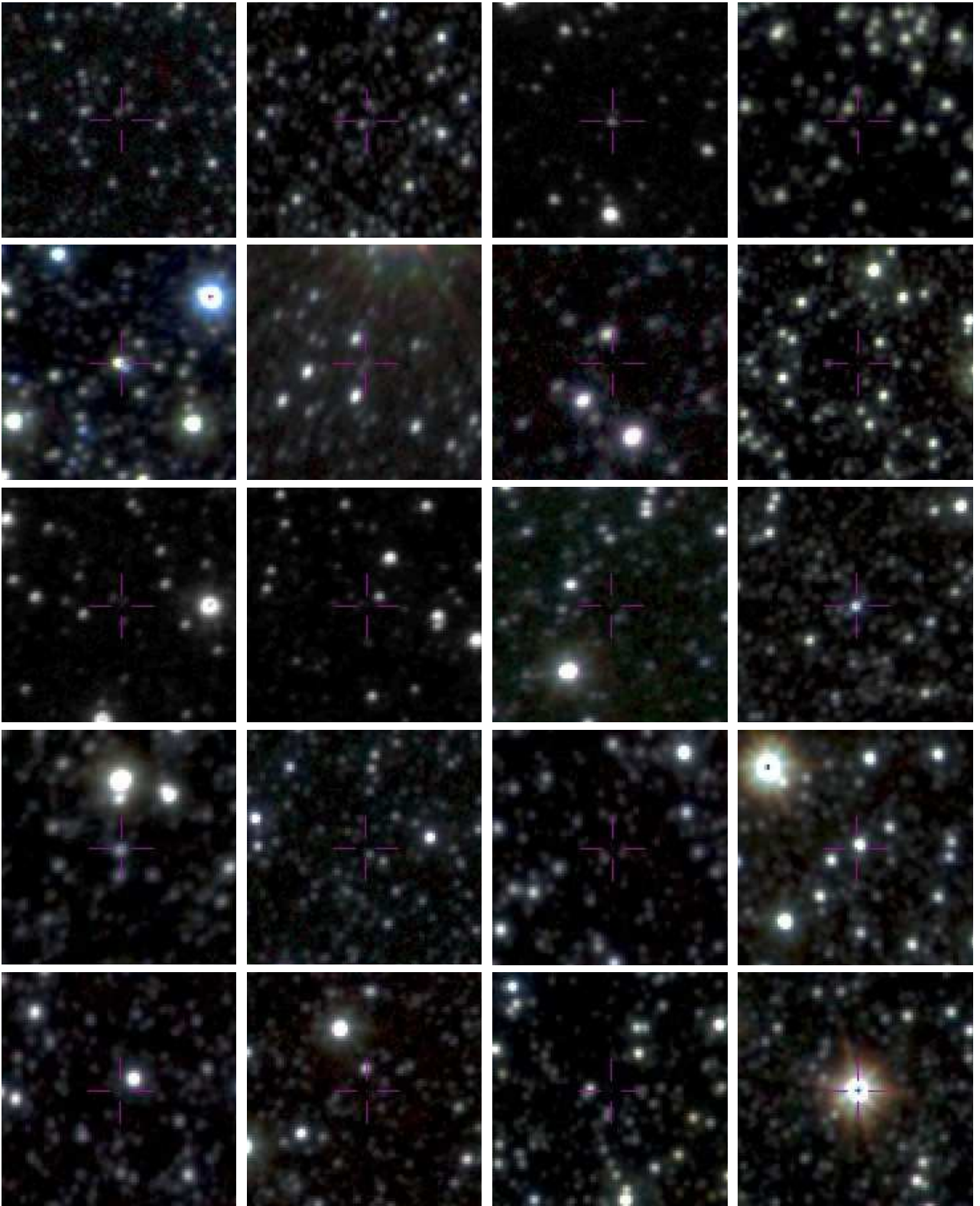


Fig. A.1. cont. First row: Nova Sgr 1932, Nova Sgr 1933, Nova Cru 1935 (K_s -band image) and Nova Sco 1935. Second row: Nova Sgr 1936, Nova Sgr 1936b, Nova Sgr 1936c and Nova Sgr 1936d. Third row: Nova Sgr 1937 (K_s -band image), Nova Oph 1940 (K_s -band image), Nova Sco 1941 and Nova Sgr 1943. Fourth row: Nova Sco 1944, Nova Sgr 1944, Nova Sgr 1945a and Nova Sgr 1945b. Last row: Nova Sgr 1947a, Nova Sgr 1948, Nova Sco 1949 and Nova Oph 1950.

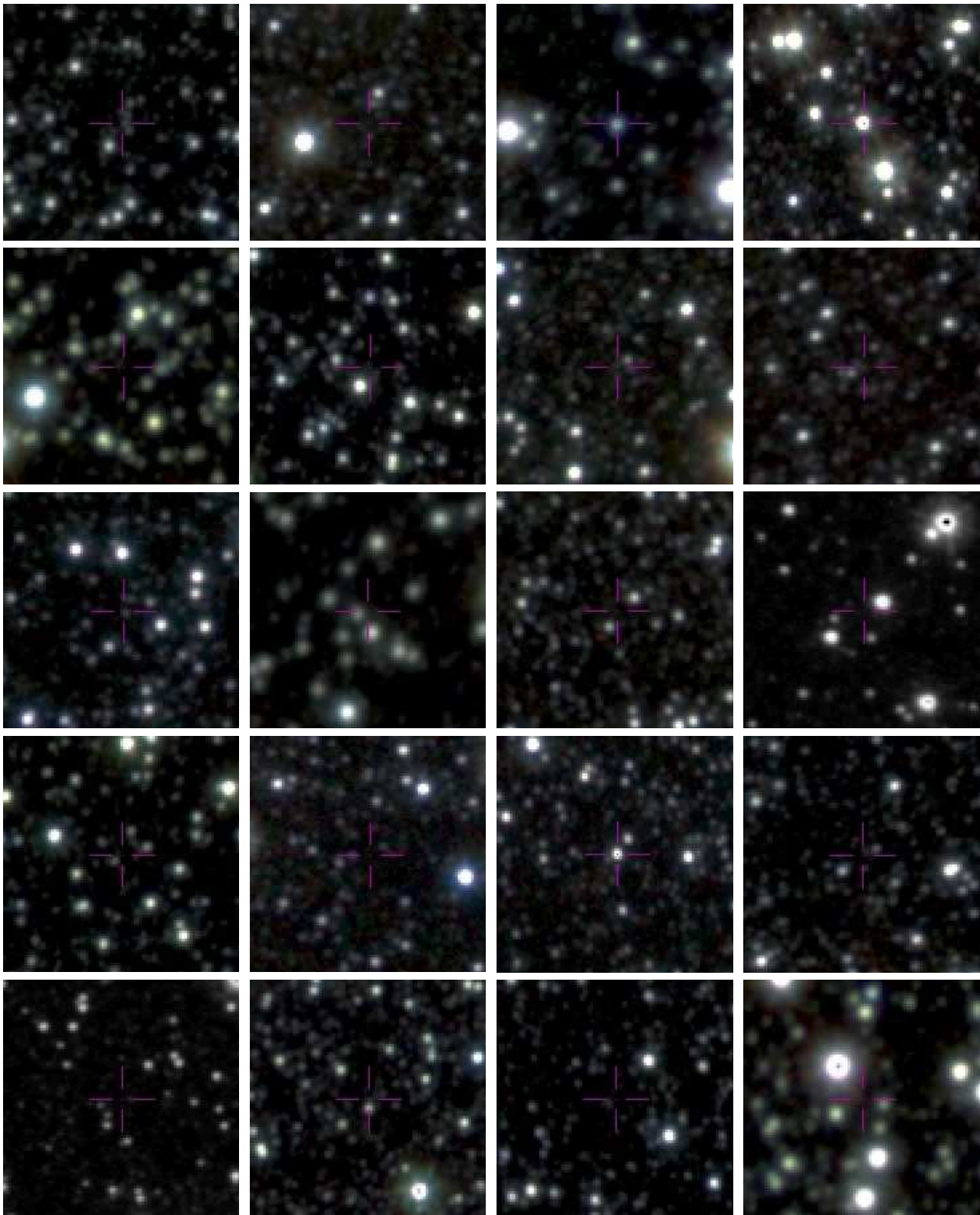


Fig. A.1. cont. First row: Nova Sco 1950a, Nova Sco 1950b, Nova Sco 1950c and Nova Sgr 1951a. Second row: Nova Sgr 1951b, Nova Sco 1952, Nova Sco 1952a and Nova Sco 1952b. Third row: Nova Sgr 1952a, Nova Sgr 1952b, Nova Sgr 1953 and Nova Oph 1954 (K_s -band image). Fourth row: Nova Sco 1954, Nova Sgr 1954a, Nova Sgr 1954b and Nova Sgr 1955. Last row: Nova Oph 1957 (K_s -band image), Nova Sgr 1960, Nova Oph 1961 and Nova Sgr 1963.

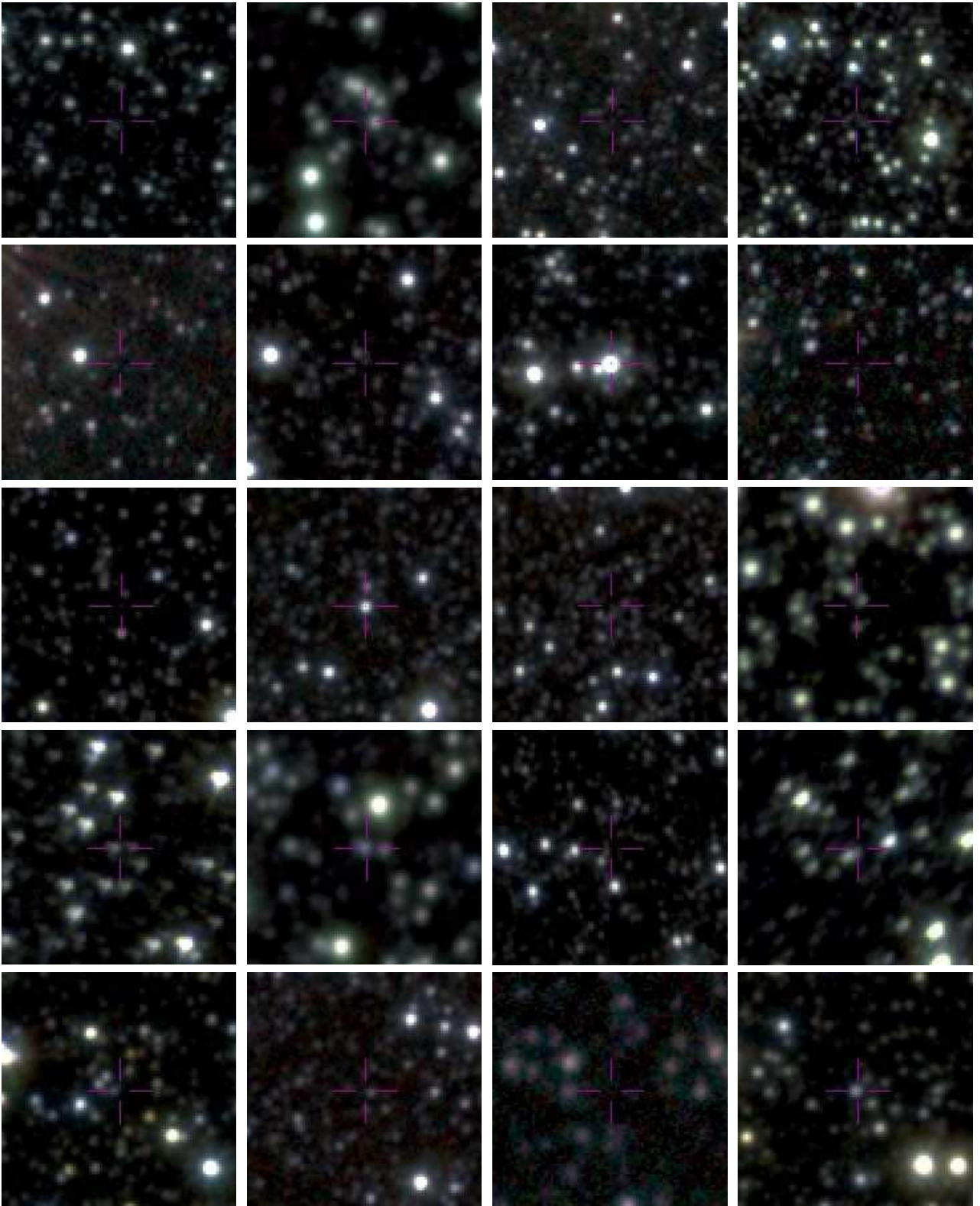


Fig. A.1. cont. First row: Nova Sco 1964, Nova Sgr 1968, Nova Sgr 1974 and Nova Sgr 1975. Second row: Nova Sgr 1977, Nova Sgr 1978, Nova Sgr 1980 and Nova Sgr 1982. Third row: Nova Nor 1983, Nova Oph 1983, Nova Sgr 1983 and Nova Sgr 1984. Fourth row: Nova Sco 1985, Nova Sgr 1986, Nova Sgr 1987 and Nova Sco 1989b. Last row: Nova Cen 1991, Nova Oph 1991b, Nova Sgr 1991 and Nova Sco 1992.

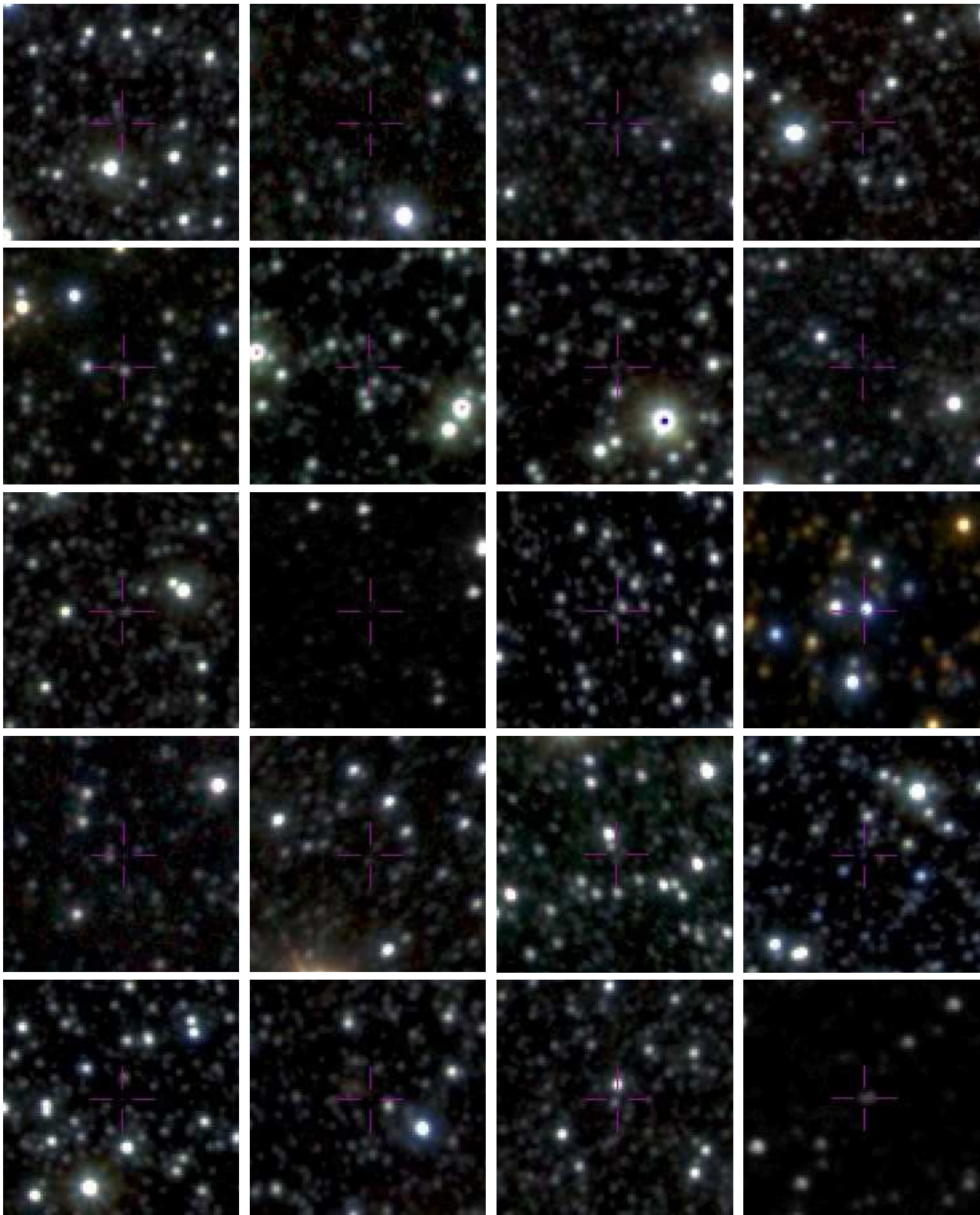


Fig. A.1. cont. First row: Nova Sgr 1992a, Nova Sgr 1992b, Nova Sgr 1992c and Nova Sgr 1993. Second row: Nova Cru 1996, Nova Sco 1997, Nova Sco 1998 and Nova Sgr 1998. Third row: Nova Sgr 1999, Nova Sgr 2000 (K_s -band image), Nova Sco 2001 and Nova Sgr 2001. Fourth row: Nova Sgr 2001b, Nova Sgr 2001c, Nova Sgr 2002 and Nova Sgr 2002b. Last row: Nova Sgr 2002d, Nova Sgr 2003b, Nova Oph 2004 and Nova Sco 2004 (K_s -band image).



Fig. A.1. cont. First row: Nova Sco 2004b, Nova Sgr 2004, Nova Cen 2005 and Nova Nor 2005. Second row: Nova Sco 2005, Nova Sgr 2005a, Nova Sgr 2005b and Nova Oph 2006. Third row: Nova Sgr 2006, Nova Oph 2007, Nova Nor 2007 and Nova Oph 2008a. Fourth row: Nova Oph 2008b (*K_s*-band image), Nova Sgr 2008, Nova Sgr 2008b and Nova Oph 2009. Last row: Nova Sgr 2009a, Nova Sgr 2009b, Nova Sgr 2009c and Nova Oph 2010.

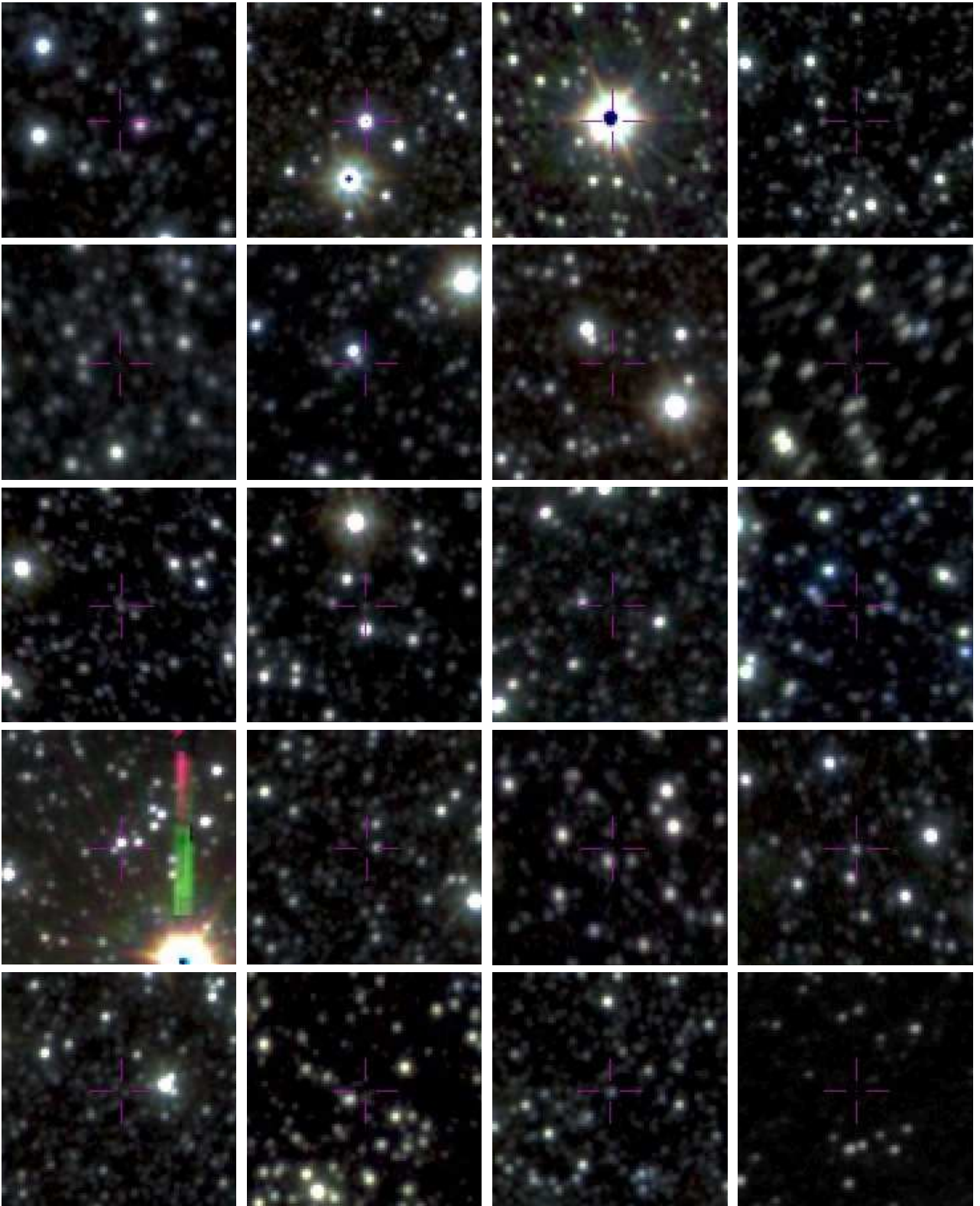


Fig. A.1. cont. First row: Nova Oph 2010b, Nova Sgr 2010, Nova Sgr 2010b and Nova Sgr 2011. Second row: Nova Sgr 2011b, Nova Cen 2012, Nova Oph 2012b and Nova Sco 2012. Third row: Nova Sgr 2012, Nova Sgt 2012c, Nova Sgt 2012d and OGLE-NOVA-001. Fourth row: V1213 Cen, PN G002.6, V0733 Sco and GR Sgr. Last row: AT Sgr, V2859 Sco, KW2003 105 and V0729 Sco.